Sabounchei Seyed Javad (Orcid ID: 0000-0001-9000-5304)

Spectral, crystallography, theoretical and antibacterial studies of palladium/ platinum(II) complexes with unsymmetrical diphosphine ylides

Seyyed Javad Sabounchei*[1]|Khadijeh Badpa[1]| Mehdi Bayat[1]|Roya Karamian[2]| Fatemeh Ghasemlou[2]| Robert W. Gable[3] | Parviz Gohari Derakhshandeh[4]|Kristof Van Hecke[4].

[1]*Faculty of Chemistry, Bu-Ali Sina University, Hamedan, 65174, Iran.*

[2]*Department of Biology, Faculty of Science, Bu-Ali Sina University, P. O. Box 65175/4161, Hamedan – Iran.*

[3]*School of Chemistry, University of Melbourne, Victoria, 3010, Australia.*

[4]*XStruct, Department of Inorganic and Physical Chemistry, Ghent University, Krijgslaan 281-S3, B-9000 Ghent, Belgium.*

*Corresponding author: jsabounchei@yahoo.co.uk (S.J. Sabounchei), Tel.: +98 8138272072; fax: +988138273231.

This is the author manuscript accepted for publication and has undergone full peer review but has not been through the copyediting, typesetting, pagination and proofreading process, which may lead to differences between this version and the Version of Record. Please cite this article as doi: 10.1002/aoc.4658

ABSTRACT: The reaction of α-keto stabilized diphosphine ylides [$Ph_2P(CH_2)_nPPh_2$=C(H)C(O)C_6H_4-*p*-CN] (n=1, (**Y^1**); n=2, (**Y^2**)) with diboromo(1,5-cyclooctadiene)palladium(II)/ platinum(II) complexes, [Pd/$PtBr_2$(cod)], in equimolar ratio gave the new cyclometalated Pd(II) and Pt(II) complexes, [$Br_2Pd(\kappa^2$-$Y^1)$] (**1**), [$Br_2Pt(\kappa^2$-$Y^1)$] (**2**), [$Br_2Pd(\kappa^2$-$Y^2)$] (**3**) and [$Br_2Pt(\kappa^2$-$Y^2)$] (**4**). These compounds were screened in a search for novel antibacterial agents and characterized successfully by FT-IR and NMR (^{1}H, ^{13}C and ^{31}P) spectroscopic methods. Also, the structure of complexes **1** and **2** were characterized with X-ray crystallography. The results showed that the P, C-chelated complexes **1** and **2** have structures consisting of five-membered rings, while **3** and **4** have a six-membered ring, formed by coordination of the ligand through the phosphine group and the ylidic carbon atom to the metal center. Also, a theoretical study on the structure of the complexes **1-4** has been investigated at the BP86/def2-SVP level of theory. The nature of metal-ligand bonds in the complexes was analyzed using EDA, and ETS-NOCV analyses. The results of EDA confirmed that the main portions of ΔE_{int}, about 57−58% in the complexes are allocated to ΔE_{elstat}.

KEYWORDS: Pd/Pt complexes; X-ray; DFT; EDA; Antibacterial activity.

1| INTRODUCTION

Unsymmetrical α-keto stabilized ylides derived from diphosphines have shown more useful application in organometallic and inorganic chemistry [1-6], especially in the synthesis of products with biological and pharmacological activities [7-9]. The development of compounds with the ability to inhibit bacterial growth has been of great interest in recent years [10]. Even though pharmacological industries have produced a number of new antibiotics in the last three decades, but resistance to these drugs by microorganisms has increased. The problem of microbial resistance is growing and the outlook for the use of antimicrobial drugs in the future is still uncertain. Therefore, actions must be taken to reduce this problem, for example, to control the use of antibiotic, develop research to better understand the genetic mechanisms of resistance, and to continue studies to develop new drugs, either synthetic or natural. The utility of metalated phosphorus ylides in synthetic chemistry has been well documented [11, 12]. The coordination and organometallic chemistry of α-keto stabilized phosphorus ylides has been investigated extensively and their ambidenticity explained in terms of a delicate balance between electronic and steric factors [13–18]. Juxtaposition of the keto group and carbanion in the phosphorus ylides causes delocalization of the ylidic electron density, and it provides additional stability in the ylide species [19-22]. Also the basicity or steric properties of the two phosphorus atoms can be different and may be used to get different coordination modes, i.e. bidendate versus monodendate [23]. Because of various coordination modes of α-keto stabilized phosphorus

ylides in metal complexes (P-, C- and P,C-coordination modes), these compounds are attractive candidates for further development in Pd/Pt- complexes [24,25]. Experimental and theoretical studies of the reactivity and coordination chemistry of carbonyl stabilized phosphorus ylides are an important research field of our group [9]. Complexes of group 10 metals (especially palladium/ platinum(II)) with phosphorus ylide ligands have attracted the interest of researchers as objects for theoretical studies. Although there is no X-ray structure available in this report to prove the molecular structure of complexes **3** and **4**, however DFT theoretical studies by using NBO, EDA and ETS-NOCV analysis have been performed to elucidate the physical and chemical nature of interactions and this is one of the purposes of this work.

Because of the similar coordination modes and chemical properties of palladium(II) and platinum(II) complexes, also the structural analogy between Pt(II) and Pd(II) complexes, encourages us to the synthesis, structural characterization, crystallography and theoretical studies of these complexes with some unsymmetrical α-keto stabilized phosphorus ylides. These ylides were coordinated to various transition metal ions such as Hg(II), Ag(I), Cu(I) and as well as Pd(II), Pt(II) [26, 27]. In this work we selected the ylides [$Ph_2P(CH_2)_nPPh_2$=C(H)C(O)C_6H_4-*p*-CN] (n=1, (**Y**^{1}); n=2, (**Y**^{2})) to participate as ligands for preparations of some cyclometal complexes. As a part of our interest in transition metal chemistry of bidentate phosphorus based ylides for cyclometalation, we concentrate on the preparation, geometric and electronic properties of a new four-coordinated Pd/Pt(II) complexes with the idea of studying its nature of metal-ligand bonds.

2 | EXPERIMENTAL

2.1| Materials and methods

All synthetic reactions were carried out under dry nitrogen using standard Schlenk techniques. 2-bromo-4'-cyanoacetophenone, dppe and dppm were purchased from commercial sources and used without further purification. [MBr_2(cod)] (M = Pd or Pt) complexes were prepared according to previously published procedures [28]. Phosphorus ylides $\mathbf{Y^1}$ and $\mathbf{Y^2}$ were synthesized and characterized previously [29]. Toluene, n-hexane and chloroform were used as reagent grade and dried over Na/Benzophenone and $CaCl_2$ subsequently. The ^{1}H, ^{13}C and ^{31}P NMR spectra were recorded on 250 MHz Bruker and 90 MHz Jeol spectrometers with $CDCl_3$ as solvents at 25 °C. IR spectra were recorded with KBr pellets using a Shimadzu 435-U 04 spectrophotometer in the region of 4000–400 cm^{-1}.

2.2 | Synthesis of Pd/Pt complexes

General procedure**:** To a dichloromethane solution of [MBr_2(cod)] (M=Pd or Pt) (0.5 mmol, 5 mL), a solution of ylide (0.5 mmol) (5 mL, CH_2Cl_2) was added. The resulting solution was stirred for 2 h at room temperature and then concentrated to a *ca.* 2 mL under reduced pressure and treated with n-hexane (5 mL) to afford the Pd/Pt complexes of desired diphosphine ylide.

2.2.1 | Data for [$PdBr_2(Ph_2PCH_2PPh_2C(H)C(O)C_6H_4$-p-CN)] (1)

Yield: 0.061 g (88%), M.p. 205 °C. Selected IR absorption in KBr (cm^{-1}) ν(CO): 1682(C=O). ^{1}H NMR (250.13 MHz, $CDCl_3$) δ_H (ppm): 4.22 (s, CH_2, 2H), 6.31 (br, 1H, PCH); 6.31–8.47 (m, 20H Ph+ 4H C_6H_4). ^{31}P NMR (101.24MHz, $CDCl_3$) δ_P (ppm): 26.05(d, PPh_2, $^{2}J_{P-P}$ = 45.45 Hz), 37.97 (d, PCH, $^{2}J_{P-P}$ = 45.45 Hz). ^{13}C NMR (62.89MHz, $CDCl_3$) δ_C (ppm): 28(s, CH_2); 38.70 (s, PCH); 118.24(s, CN); 121.34-140.32 (m, Ph); 194.79(s, CO).

2.2.2 | Data for [$PtBr_2(Ph_2PCH_2PPh_2C(H)C(O)C_6H_4$-p-CN)] (2)

Yield: 0.050 g (80%), M.p. 200 °C. IR (KBr disk) ν(cm^{-1}): 1685 (C=O). ^{1}H NMR (250.13 MHz, $CDCl_3$) δ_H (ppm): 4.28 (br, 2H, CH_2); 4.91 (t, H, PCH); 6.94–7.85 (m, 20H Ph+ 4H C_6H_4). ^{31}P NMR (101.24MHz, $CDCl_3$) δ_P (ppm): 5.78 (td, PPh_2,$^{1}J_{Pt-P}$ = 1928.09 Hz); 42.95 (d, PCH, $^{2}J_{P-P}$ = 41.41 Hz). ^{13}C NMR (62.89MHz, $CDCl_3$) δ_C (ppm): 38.70 (s, CH_2); 46.22 (m, PCH); 118.07(s, CN); 127.60–134.21(m, Ph); 192 (s, CO).

2.2.3 | Data for [$PdBr_2(Ph_2P\ CH_2CH_2PPh_2C(H)C(O)C_6H_4$-p-CN)] (3)

Yield: 0.051 g (85%), M.p. 201 °C. Selected IR absorption in KBr (cm^{-1}) ν(CO): 1626(C=O). ^{1}H NMR (250.13 MHz, $CDCl_3$) δ_H (ppm): 4.22 (br, 4H, CH_2); 6.31 (s, 1H, PCH); 7.16–8.47 (m, 20H Ph+ 4H C_6H_4).^{31}P NMR (101.24MHz, $CDCl_3$) δ_P (ppm): 23.59 (d, PPh_2, $^{2}J_{P-P}$ = 23.23 Hz); 28.17 (d, PCH, $^{2}J_{P-P}$ = 22.22 Hz). ^{13}C NMR (62.89MHz, $CDCl_3$) δ_C (ppm): 22.96(s, CH_2); 30.33(s, PCH); 118.24 (s, CN); 121.34-140 (m, Ph); 194.61(s, CO).

2.2.4 | Data for [$PtBr_2(Ph_2P\ CH_2CH_2PPh_2C(H)C(O)C_6H_4$-p-CN)] (4)

Yield: 0.060 g (95%), M.p. 200-205 °C. IR (KBr disk) ν(cm^{-1}): 1628(C=O). ^{1}H NMR (250.13 MHz, $CDCl_3$) δ_H (ppm): 3.7 (m, 4H, CH_2); 6.47 (br, 1H, PCH); 7.125–8.66 (m, 20H Ph+ 4H C_6H_4). ^{31}P NMR (101.24MHz, $CDCl_3$) δ_P (ppm): 6.48 (td, PPh_2, $^{1}J_{Pt-P}$ = 3910.89Hz); 20.14 (td, PCH, $^{2}J_{P-P}$ = 153.5Hz). ^{13}C NMR (62.89MHz, $CDCl_3$) δ_C (ppm):38.90 (s, CH_2); 45.66 (s, PCH); 118.24 (s, CN); 127.20-140.86 (m, Ph); 194.50(s, CO).

2.3 | Crystallography

Single crystals of **1** and **2** were crystallized by slow evaporation from dichloromethane solution. A suitable crystal was selected and mounted on a SuperNova, Dual, Cu at zero, Atlas diffractometer. The crystal was kept at 130.00(10) K during data collection. Using Olex2 [30], the structure was solved with the ShelXT [31] structure solution program using Intrinsic Phasing and refined with the ShelXL [32] refinement package using Least Squares minimisation.

2.4 | Computational studies

A computational study on structures and nature of metal-ligand (Y= $\mathbf{Y^1}$ and $\mathbf{Y^2}$) bonds in some complexes of five- and six-membered rings P, C-chelated complexes of Pd(II) and Pt(II) with general formula [YMBr2](M=Pd, Pt Y= $\mathbf{Y^1}$, $\mathbf{Y^2}$) has been reported. The geometries of the complexes have been optimized at BP86 [33, 34] /def2-SVP [35] level of theory. Vibrational frequency analyses, calculated at the same level of theory, indicate that the optimized structures are at the stationary points corresponding to local minima without any imaginary frequency. All calculations were performed using the Gaussian 09 set of programs [36]. It has been shown that

in former studies the BP86 is a suitable level for calculation of bonding situation between the M←L in such as these complexes [37-52]. For bonding analyses, the terms of EDA were carried out at BP86/TZ2P(ZORA)//BP86/def2-SVP with C1 symmetry. The basis sets for all elements have triple-ζ quality augmented by one set of polarization functions (ADF basis set TZ2P (ZORA)) with the program package ADF2009.01.

2.5 | Antibacterial activity

The antimicrobial effect of the new samples was assessed by disc diffusion method [53]. Paper discs (6.4 mm in diameter) were submerged in the sample solutions. The samples were dissolved in DMSO to make a 1 mg ml^{-1} solution and other concentration make from this concentration, and then apply on the blank sterile paper discs. Dried discs were placed onto Muller-Hinton agar medium that previously inoculated with a bacterial suspension (1.5×10^8 bacteria/ml). The cultures were incubated at 37 ^oC for 24 h. Antibacterial activity of the new samples were evaluated against 2 gram positive, namely *Staphylococcus aureus* (ATCC 25923) and *Bacillus subtilis* (PTCC 1247) and 2 gram negative *Escherichia coli* (ATCC 35218) and *Pseudomonas aeruginosa* (ATCC 27853) at 2 different concentrations (1 and 0.5 mg ml^{-1}). The antibacterial activity against each test organism was quantified by determining mean zone of inhibition. Negative controls were prepared by using DMSO. Gentamicin, Penicillin and Streptomycin were used as positive reference standards.

2.5.1 | Statistical analyses

All data from antibacterial tests are the average of triplicate analyses. Analysis of variance was performed by Excel and SPSS procedures statistical analysis was performed using Duncan's test and P value < 0.05 was regarded as significant.

3| RESULTS AND DISCUSSION

3.1 | Synthesis

Reaction of ligands $\mathbf{Y^1}$ and $\mathbf{Y^2}$ with [MBr_2(cod)] (M = Pd /Pt) in equimolar ratio yielded the new P,C-chelated pallada- and platinacycle [$MBr_2(Ph_2P(CH_2)_nPPh_2C(H)C(O)C_6H_4$-*p*-CN)] (n= 1, M=Pd **(1)** , n=1, M=Pt, **(2)** , n=2, M=Pd, **(3)**andn=2, M=Pd, **(4)**) in 80-95% yields (Scheme 1). All complexes are soluble in chloroform and dichloromethane and insoluble in non-polar solvents, such as n-hexane and petroleum ether.

SCHEME 1

3.2 | Characterization

The structure of products was characterized successfully by ^{1}H, ^{13}C and ^{31}P NMR spectroscopic methods and other techniques as well as IR and X-ray. Table 1 shows the brief summary of these collected data sets. Also, the exact structure of complexes **1** and **2** with atomic resolution were being unequivocally determined by single crystal X-ray diffraction technique.

TABLE 1

3.2.1 | Infra-red spectra

As noted in the literature [54], coordination of ylide through the carbon (chelating mode) causes a significant increase in the ν CO frequency. IR spectra of complexes **1-4** show a significantly frequency shift of ν(CO) than those of the related phosphorus ylides $\mathbf{Y^1}$and $\mathbf{Y^2}$. These observations are in agreement with the chelation of ylides through the P and Cα atoms. Presence of ν CO bands around 1600 cm^{-1} in the IR spectra of these complexes indicates that products (P, C-chelated complexes) were formed. Furthermore, the IR spectra of complexes **1-4** were not shown the ν CO bands around 1500 cm^{-1}, this confirme that there are not any significant amounts of P, P-coordinated complexes as side products.

3.2.2 | NMR spectral data

Coordination of phosphorus ylides as P,C-chelated form can makes a large chemical shift for both free (PPh_2) and bonded (PCH) phosphorus atoms. While, in P, P- coordinated form it was only the signal of PPh_2 moiety was shifted to higher frequencies. The ^{31}P NMR chemical shift values for all complexes appear to be shifted downfield with respect to all parent ylides, indicating that coordination of the ylides has occurred. The ^{31}P NMR spectrum of complex **1** shows two doublet peaks around δ= 26.05 and 37.97 ppm, which is assigned to PPh_2 ($\mathbf{P_a}$) and PCH ($\mathbf{P_b}$), respectively (Fig. 1), whereas the ^{31}P NMR spectrum of complex **2** shows two doublet peaks around δ= 5.78 ppm along with two satellite peaks due to ^{195}Pt-^{31}P coupling and 42.95 ppm, which is assigned to PPh_2 ($\mathbf{P_a}$) and PCH ($\mathbf{P_b}$), respectively (Fig. 1). The ^{31}P NMR spectrum of complex **3** shows two doublet peaks around δ=23.59 and 28.17 ppm, which is assigned to PPh_2 and PCH, respectively (Fig.S9, shown in supporting information).^{31}P NMR spectrum of

complex **4** shows a different pattern as two doublet peaks around δ= 6.48 and 20.14 ppm, along with two satellite peaks due to ^{195}Pt-^{31}P coupling, which is assigned to PPh_2 and PCH, respectively (Fig.S13, shown in supporting information).

FIG 1

The ^{1}H NMR chemical shift values for these complexes appear to be shifted downfield with respect to the parent ylide, indicating also that the coordination of the ylide through P and Cα atoms has occurred. The ^{1}H NMR spectra of P, C-chelated complexes **1**-**4** (Fig.S2, Fig.S6, Fig.S10 and Fig.S14 supporting information) exhibited characteristic shifts in the methinic proton signals. This is interesting, because complexation of the ylides **(Y^1/ Y^2)** to Pd/Pt through free phosphorus atom was not change significantly the chemical shift values of ^{1}H NMR. While, coordination through carbanion causes the shift of PCH peaks to higher frequency around 4.91-6.47 ppm. The ^{1}H NMR spectra of complexes **1**-**4** show the signal of the methinic proton as a broad peak around 6 ppm due to the coupling with the neighbor phosphorus atoms.

The ^{13}C NMR spectra of complexes **1** and **2** (Fig.S3, Fig.S7, supporting information) showed downfield shift of CO, PCH and PCH_2 groups in the respect to the parent ylide $\mathbf{Y^1}$. Chemical shift values in the ^{13}C NMR spectra of complexes **3** and **4** (Fig.S11, Fig.S15, supporting information), showed significant shift in comparison to the parent ylide $\mathbf{Y^2}$. This observation was also confirmed that coordination of ylides $\mathbf{Y^1}$ and $\mathbf{Y^2}$ were occurred through the P,C-coordination sites.

3.3 | Crystallography

The single crystals of **1** and **2** were crystallized by slow evaporation from dichloromethane. The molecular structures of **1** and **2** were shown in Fig. 2. Relevant parameters concerning data collection and refinement were given in Table 2. Selected bond distances and angles for the unit cells of **1** and **2** are displayed in Table 3. (See supporting information, Table.S1-S15).

FIG. 2

TABLE 2

TABLE 3

The structure of samples **1** and **2** are as proposed. The Pt/Pd are in a slightly distorted square planar environment, coordinated by two bromine atoms one phosphorous atom and one ylidic carbon atom, the four coordinating atoms show a slight tetrahedral distortion with a rms deviation of 0.139 Å. The five-membered ring formed by the coordination of the ligand to the platinum is in an envelope conformation, with C1 lying 0.820(3) Å out of the plane of the other four atoms Pt1, P2, P3 & C22. The Pt-Br distance trans to the ylidic carbon atom, 2.4625(3) Å, is slightly shorter than the corresponding distance trans to the phosphorous atom, 2.4912(3) Å. The dihedral angle between the keto group and the cyano-substitited aromatic ring is 16.1(2)°. The structure is similar to other Pd ylide complexes, such as dichloro-(1-(((diphenylphosphino) methyl) (diphenyl) phosphonio)-2-(2-naphthyl)-2-oxoethyl)-palladium(II) [55] and (2-(biphenyl-

4-yl)-1-(((diphenylphosphino)methyl)-(diphenyl)phosphonio)-2-oxoethyl)-(dichloro)-palladium [29].

Crystal Data for $C_{34}H_{27}Br_2NOP_2Pd$ (M =793.71 g/mol): monoclinic, space group C2/c (no. 15), a = 22.9998(5) Å, b =15.4956(3) Å, c = 18.4400(3) Å, β = 108.290(2)°, V = 6239.9(2) Å3, Z = 8, T = 100.0(1) K, μ(MoKα) = 3.287 mm^{-1}.

3.4 | Theoretical studies

A computational study on structures and nature of metal-ligand (Y→M) bonds in [$YMBr_2$] (M=Pd, Pt Y=**Y**^{1}, **Y**^{2}) complexes has been reported at the BP86 level of theory using def2-SVP basis set. The structural data obtained in this work (See Fig. 4) show that the **Y**^{1} complexes of Pd and Pt are formed the monomeric P, C chelate complexes with five-membered rings which lying square planar geometry around the metal center. Also, this work and previous experimental data [39] confirm that, upon complexation of the **Y**^{1} and **Y**^{2} ligands, the monomeric P, C chelate complexes are formed as five- and six-membered rings with a square planar geometry around the metal center.

The optimized structures of the [YMBr2](M=Pd, Pt Y= **Y**^{1}, **Y**^{2}) complexes at BP86/Def2-SVP are shown in Fig. 3 and the trends for the variation of the corresponding bond lengths and bond angles and their comparison with experimental data are given in Table 4. (See supporting information, Table.S16-S19). The result in good agreement with experiment and also our recent work [40] show that changing the ligand from **Y**^{1} to **Y**^{2} and M atom from Pd to Pt have an insignificant effect on the values of C→M and P→M bond lengths. Also, the calculated and

experimental C→M and P→M bond lengths in the complexes are in ranges of 2.09−2.14Å and 2.20−2.29Å respectively.

On the other hand, the P−M−C bond angle in six-membered rings complexes is greater than five -membered rings complexes. (See Fig.3 and Table 4).

FIG. 3

TABLE 4

Morokuma [56] and Ziegler [57] developed EDA in the 70's. With the help of this technique, a quantitative computational pattern for the explanation of the strength of M←L σ donation, and M→L back bonding in the main group and transition metal complexes with different types of ligands is in hand [37-52, 58-62].

In continuation, through the energy decomposition analyses (EDA), the strength and nature of donor−acceptor bonds between the phosphorus ylides (Y=$\mathbf{Y^1}$, $\mathbf{Y^2}$) and MBr_2 fragment have been investigated at BP86/TZ_2P(ZORA)//BP86/def2-SVP with C1 symmetry using the program package ADF2009.01.

The results of EDA for all of the aforementioned complexes are given in Table 5. In the EDA, the bonding formation of interacting fragments would result from 4 main components as follows:

$$\Delta E_{int} = \Delta E_{elstat} + \Delta E_{Pauli} + \Delta E_{orb} + \Delta E_{disp}$$

Where ΔE_{elstat} is electrostatic interaction, ΔE_{Pauli} is Pauli repulsion, ΔE_{orb} is orbital interaction, and ΔE_{disp} is dispersion energy between two fragments.

TABLE 5

The results of EDA confirm that the main portions of ΔE_{int}, about 57−58% in the complexes are allocated to ΔE_{elstat} (see Table 5).

Also, the visualization of natural orbitals for chemical valence NOCV pairs (Δρ) between the donor orbitals of phosphorus ylides (Y=$\mathbf{Y^1}$, $\mathbf{Y^2}$) and the acceptor orbitals of the MBr_2 fragment are shown in Figs. 4 and 5. As can be seen, the dominant term of ΔE_{orb} for all of the aforementioned complexes arises from σ-orbital interactions (Δρ1, Δρ2). The calculated data show that the σ-orbital interactions account for 77%- 80% of the ΔE_{orb} term for studied complexes. Also, the shapes of the orbital pairs of Δρ3, Δρ4 and Δρ5 refer to π back-donations which are in plane and out of plane and accounts for about 20% -23% of ΔE_{orb} term (See Table 5 and Figs.4 and 5).

FIG. 4

FIG. 5

3.5 | Antibacterial activity

Antibacterial activity of the samples were evaluated against 2 gram negative and 2 gram positive bacteria, namely *E. coli*, *P. aeruginosa*, *S. aureus* and *B. cereus* by disc diffusion method at 2 different concentrations. It is well known that *S. aureus*, *E. coli* and *Bacillus* species are food poisoning agents [63, 64]. The solvent DMSO, which was screened as a negative

control against all bacteria had no activity. Results from antibacterial assessment are presented in Tables 6 and 7. Antibacterial property of the samples showed the acceptable concentration-dependent in comparison with some positive controls. It was shown that the biological activity of a compound is mainly attributed to its major components, and also the synergistic or antagonistic effect of its components in a minor percentage of the reaction mixture [65]. Antibacterial activity of the samples especially the Pd complex compared to the reference antibiotics was found to be good. The presence of Pd groups exerts a number of changes on antibacterial activity between the tested complexes (Table 6). The complexes **3** and **4**, which is modified structures of the sample **1** showed high antibacterial activity. The results revealed that the complexes exhibits similar and even higher antibacterial activity than those of similar Pd/Pt(II) complexes [9, 66, 67]. On the whole, based on the results of antibacterial experiments and comparative study, it can be concluded that the metal ions have important effect on antibacterial activity and also primary ligands can exert additional effects on the antibacterial.

In addition, *S. aureus* was the most sensitive bacteria to the samples in both concentrations, while *E. coli* was the most insensitive bacterium. The antibacterial activity was more pronounced on the gram-positive bacteria (*S. aureus* and *B. cereus*) than the gram-negative ones (*E. coli* and *P. aeruginosa*). The reason for the difference in sensitivity between them might be ascribed to the differences in morphological constitutions between these microorganisms. The gram-negative bacteria have an outer phospholipidic membrane carrying the structural lipopolysaccharide components. This makes the cell wall impermeable to antimicrobial chemical

substances. The gram-positive bacteria on the other hand are more susceptible having only an outer peptidoglycan layer, which is not an effective permeability barrier. Therefore, the cell walls of gram-negative organisms act as a diffusion barrier and making them less susceptible to the antimicrobial agents than aerogram-positive bacteria [68, 69]. In spite of this permeability differences, however, some of the samples have still exerted some degree of inhibition against gram-negative organisms as well.

TABLE 6

TABLE 7

Therefore, our results revealed that the newly synthesized complexes have great potential as antimicrobial compounds against microorganisms. Thus, they may be used in the treatment of infectious diseases caused by resistant microbes. The synergistic effect of the association of antibiotic with the samples against resistant bacteria leads to new choices for treatment of infectious diseases.

4 | CONCLUSION

The present study describes the synthesis and characterization of a series of chelate Pd/Pt(II) complexes derived from Pd/$PtBr_2$cod and a bifunctionalized phosphorus ylide ($\mathbf{Y^1}$and $\mathbf{Y^2}$) by simple and convenient synthetic methods in satisfactory yields. On the basis of the physicochemical and spectroscopic data, we propose that ligands herein exhibit bidendate P, C-coordination to the metal centre, which is further confirmed by the X-ray crystal structure of the complexes **1** and **2**. The nature of metal-ligand bonds in the complexes was analyzed using EDA,

and the extended transition state combined with the natural orbitals for chemical valence (ETS-NOCV). The results of EDA confirm that the main portions of ΔE_{int}, about 57−58% in the complexes are allocated to ΔE_{elstat}. Also, the ETS-NOCV analyses confirm that the NOCV pairs ($\Delta\rho$) between the donor orbitals of phosphorus ylides (Y=$\mathbf{Y^1}$, $\mathbf{Y^2}$) and the acceptor orbitals of MBr_2 fragments arises from σ-orbital σ-orbital interactions (about 77%- 80%) and π back-donation (about 20% -23%) to the ΔE_{orb} term respectively. Furthermore these compounds exhibited excellent biological activities.

Acknowledgements

Funding of our research from the Bu-Ali Sina University is gratefully acknowledged.

Supplementary material

Physical measurements and selected ^{31}P, ^{13}C and ^{1}H NMR spectra of some compounds can be found in the online version. CCDC 1552702 and 1548313 contains the supplementary crystallographic data for the complexes **1** and **2**, respectively. These data can be obtained free of charge via www.ccdc.cam.ac.uk/data_request/cif or from the Cambridge Crystallographic Data Center, 12, Union Road, Cambridge CB2 1EZ, UK. Tel.: +44 0 1223 762911; or deposit@ccdc.cam.ac.uk.

REFERENCES

[1] M.I. Bruce, B.G. Ellis, P. J. Low, B.W. Skelton and A. H. White, *Organometallics*. **2003**, 22, 3184-3198.http://pubs.acs.org/doi/abs/10.1021/om030015g

[2] M.J. Joshi, S.J. Thornburn, S.J. Retting, B.R. James, *Inorg. Chim. Acta*. **1992**, 283, 198-200.

[3] O. Lavastre, M. Even and P.H. Dixneuf, *Organometallics*. **1996**, 15, 1530–1531.

[4] M.P. Cifuentes, C.E. Powell, M.G. Humphrey, G.A. Heath, M. Samoc and B. Luther-Davies, *J. Phys. Chem*. **2001**, 105, 9625-9627.

[5] H. Aneetha, M. Jimenez-Tenorio, M.C. Puerta and P. Valerga, *Organometallics*. **2003**, 22, 1779–1782.

[6] Y.B. Kang, M. Pabel, D.D. Pathak, A.C. Willis, S.B. Wild, *Main Group Chem*. **1995**, 8998.

[7] S.J. Sabounchei, A. Hashemi, A. Yousefi, P. Gohari Derakhshandeh, R. Karamian, M. Asadbegy, K. Van Hecke, *Polyhedron*. **2017**, 135, 1-9

[8] S.J. Sabounchei, S. Samiee, M. Pourshahbaz, S. Salehzadeh, M. Bayat, D. Nematollahi, R. Karamian, M. Asadbegy, *J. Chemic. Res*. **2014**, 38, 1-64.

[9] S.J. Sabounchei, M. Ahmadi, Z. Nasri, E. Shams,S. Salehzadeh, Y. Gholiee, R. Karamian, M. Asadbegy , S. Samiee, *C. R. Chimie*. **2013**, 16, 159–175.

[10] P. M. Bennett, *Br. J. Pharmacol*. **2008**, 153, S347–S357.

[11] O.I. Kolodiazhnyi, *Tetrahedron*. **1996**, 52, 1855.

[12] N.A. Nesmeyanov, V.M. Novikov, Q.A. Reutov, *J. Organomet. Chem.* **1965**, 4, 202.

[13] W.C. Kaska, *Coord. Chem. Rev*. **1983**, 48, 1.

[14] U. Belluco, R.A. Michelin, M. Mozzon, R. Bertani, G. Facchin, L. Zanotto, L. Pandolfo, *J. Organomet. Chem*. **1998**, 557, 37.

[15] L.R. Falvello, S. Fernandez, R. Navarro, A. Rueda, E.P. Urriolabeitia, *Inorg. Chem*. **1998**, 37, 6007.

[16] R. Navarro, E.P. Urriolabeitia, *Dalton Trans*. **1999**, 4111.

[17] H. Schmidbaur, *Angew. Chem*. **1983**, 22, 907.

[18] L.R. Falvello, S. Fernandez, R. Navarro, A. Rueda, E.P. Urriolabeitia, *Organometallics*. **1998**, 17, 5887.

[19] M.M. Ebrahim, H. Stoeckli-Evans, K. Panchanatheswaran, *Polyhedron*. **2007**, 26, 3491.

[20] K. Karami, C. Rizzoli, F. Borzooie, *Polyhedron*. **2011**, 30, 778.

[21] J. Vicente, M.T. Chicote, J. Fernandez-Baeza, J. Martin, I. Saura-Llamas, J. Turpin, P.G. Jones, *J. Chem. Soc*. **1987**, 409-421.

[22] J. Vicente, M.T. Chicote, M.C. Lagunas and P.G. Jones, *Dalton Transactions*. **1991**, 10.

[23] R.E. Cramer, S. Roth, F. Edelmann, M.A. Bruck, K.C. Cohn, J.W. Gilje, *Organometallics*. **1989**, 8, 1192–1199.

[24] E.PUrriolabeitia, *Dalton Trans.* **2008**, 42, 5673–5686.

[25] J.Vicente, M.T.Chicote, J.Fernhdez-Baeza, F.J.Lahoz, and J.A.Ldpez, *AmericanChemical Society.* **1991**.

[26] S.J. Sabounchei, M. Zamanian, M.Pourshahbaz, M. Bayat, Roya Karamian, M. Asadbegy, *J. Chem. Res*. **2016**, 40, 130.

[27] S. J. Sabounchei, S. Samiee, S. Salehzadeh, Z. B. Nojinib and E. Irranc, *J. Organomet. Chem*. **2010**, 695, 1441–1450.

[28] D. Drew, J. R. Doyle, *Inorg. Synth*. **1985**, 13, 1163.

[29] S.J. Sabounchei, M. Panahimehr, M. Ahmadi, Z. Nasri, H.R. Khavasi, *J.Organomet.Chem*. **2013**, 723, 207.

[30] O.V. Dolomanov, L.J. Bourhis, R.W. Grosse-Kunstleve, P.D. Adams, R.J. Gildea, J.A.K. Howard and H. Puschmann, *j. Appl. Crystallo*. **2011**, 44, 1259-1263.

[31] G.M. Sheldrick, *Acta Crystallogr. C*. **2015**, C71, 3-8.

[32] G.M. Sheldrick, *Acta Crystallogr A*. **2015**, A71, 3-8.

[33] A.D. Becke, *Phys. Rev. A*. **1988**, 38, 3098-3100.

[34] J.P. Perdew, *Phys. Rev. B*. **1986**, 33, 8822-8824.

[35] A. Schafer, H. Horn, R. Ahlrichs, *J. Chem. Phys*. **1992**, 97, 2571.

[36] M.J. Frisch, et al., Gaussian 09, Revision A.02. Gaussian, Inc, *Wallingford CT*. **2009**.

[37] S.J. Sabounchei, M. Pourshahbaz, S. Salehzadeh, M. Bayat, R. Karamia, M. Asadbegy, H. R. Khavasi, *Polyhedron*. **2015**, 85, 652.

[38] S.J. Sabounchei, H. Nemattalab, S. Salehzadeh, S Khani, M. Bayat, H.R. Khavasi, *Polyhedron*. **2008**, 27, 2015.

[39] S.J. Sabounchei, M. Sayadi, M. Bayat, A. Sedghi, R.W. Gable, *J. Coord. Chem*. **2017**, 70.doi.org/10.1080/00958972.2017.1397640

[40] H. Keypour, M. Rezaeivala, A. Ramezani-Aktij, M. Bayat, N. Dilek, H. Unver, *Mol. Struc*. **2016**, 1115, 180.

[41] M. Bayat, M. Hatami, *Polyhedron*. **2016**, 110, 46.

[42] S.J. Sabounchei, A. Yousefi, M. Ahmadianpoor, A. Hashemi, M. Bayat, A. Sedghi, F.A. Bagherjeri, R.W. Gable, *Polyhedron*. **2016**, 117, 273.

[43] H. Keypour, M. Liyaghati-Delshad, M. Rezaeivala, M. Bayat, *J Iran Chem Soc*. **2015**, 621.

[44] S.J. Sabounchei, M. Ahmadianpoor, A. Yousefi, A. Hashemi, M. Bayat, A. Sedghi, F. Akhlaghi Bagherjeri, R. W. Gable, *RSC Adv*. **2016**, 6, 28308.

[45] S. Salehzadeh, M. Khalaj, S. Dehghanpour, M. Bayat, *J. Iran Chem. Soc*. **2014**, 23 11, 9.

[46] M. Bayat, F. Amraie, S. Salehzadeh, *J. Theor.Comp. Chem*. **2016**, 15, 16500321.

[47] S.J. Sabounchei, M. Sarlakifar, S. Salehzadeh, M. Bayat, M. Pourshahbaz, H. R. Khavasi, *Polyhedron*. **2012**, 38, 131.

[48] M. Bayat, M. von Hopffgarten, S. Salehzadeh, G. Frenking, *J. Organomet. Chem*. **2011**, 696, 2976.

[49] M. Bayat, S. Salehzadeh, G. Frenking, *J. Organomet. Chem*. **2012**, 697, 74.

[50] M. Bayat, N. Ahmadian, *Polyhedron*. **2015**, 96, 95.

[51] M. Bayat, N. Ahmadian, *J. Iran. Chem. Soc.* **2016**, 13, 397.

[52] M. Bayat, A. Sedghi, L. Ebrahimkhani, S.J. Sabounchei, *Dalton Trans*. **2017**, 46, 207.

[53] A.W. Bauer, W.M.M.Kirby, J.C. Sherries, M.Turck, Am. *J. Clin. Pathol*. **1966**, 45, 493-496.

[54] M. Kalyanasundari, K. Panchanatheswaran, W.T. Robinson, H.Wen, *Organomet Chem*. **1995**, 491, 103.

[55] S.J. Sabounchei, M. Hosseinzadeh, M. Panahimehr, D. Nematollahi, H.R. Khavasi, S. Khazalpour, *Transition Met.Chem*. **2015**, 40, 657.

[56] K. Morokuma, Theor. *J. Chem. Phys*. **1971**, 55, 1236.

[57] T. Ziegler, A. Rauk, *Theor. Chim. Acta*. **1977**, 46, 1.

[58] G. Frenking, K. Wichmann, N. Frohlich, C. Loschen, M. Lein, J. Frunzke, V.c.M. Rayon, *Coord. Chem. Rev*. **2003**, 55, 238–239.

[59] M. Lein, A. Szabo, A. Kovacs, G. Frenking, *Farad. Dis*. **2003**, 124, 365.

[60] M. Lein, G. Frenking, *Chapter 13, Elsevier, Amsterdam*. **2005**, 291.

[61] M. Bayat, S. Kamali, *J. Mol. Liq*. **2016**, 222, 953.

[62] M. Bayat, E. Soltani, *Polyhedron*. **2017**, 123, 39.

[63] B. Aldona, S. Raymond, *Informa Health Care, CRC Press*. **1994**, 83-84.

[64] S. Burt, *Int. J. Food Microbiol*. **2004**, 94, 223-253.

[65] J.E. Gray, P.R. Norton, R. Alnouno, C.L. Marolda, K. Valvano, M.A. Griffiths. *Biomater*. **2003**, 24, 27-59.

[66] S. J. Sabounchei, P. Shahriary, S. Salehzadeh,Y. Gholiee, A. Chehregani, *C. R. Chimie*. **2015**, 18, 564-572.

[67] P.A. Ajibade and O.G. Idemudia, Bioinorg. *Chem. Appl.* **2013**, 8.

[68] N.Hodges. M.E. Aulton, *Pharmaceutics*. **2002**, 606.

[69] A. Nostro, M.P. Germano, V. Angelo, A. Marino, M.A. Cannatelli, *Lett. Appl. Microbiol.* **2000**, 30, 379-384.

Table 1 Spectroscopic data for compounds **Y^1, Y^2** and **1-4.**

Compound	IR; ν(CO) cm^{-1}	^{1}H NMR; δ(PCH) ppm	^{13}C NMR; δ(CO) ppm	^{31}P NMR; δ(PCH) and (PPh_2) ppm
Y^1	1572	4.33	183.18	15.35, -29.48
1	1682	6.31	194.79	37.97, 26.05
2	1685	4.91	192	42.95, 5.78
Y^2	1570	4.26	188.79	17.18, -12.83
3	1626	6.31	194.61	28.17, 23.59
4	1628	6.47	194.50	20.14, 6.48

Table 2 Crystal data and structure refinement for **1** and **2**.

Empirical formula	C34H27Br2NOP2Pd	C34H27Br2NOP2Pt
Formula weight	793.71	882.41
T [K]	100.0(1)	130.00(10)
Crystal system	Monoclinic	Monoclinic
Space group	C2/c	C2/c
a [Å]	22.9998(5)	23.0102(3)
b [Å]	15.4956(3)	15.52552(20)
c [Å]	18.4400(3)	18.4538(2)
α [°]	90	90
β [°]	108.290(2)	108.0847(14)
γ [°]	90	90

V [Å^3]	6239.9(2)	6266.85(15)
Z	8	8
D_c [Mg m^{-3}]	1.690	1.871
μ [mm $^{-1}$]	3.287	12.550
F(000)	3136.0	3392.0
λ (Mo-K$_\alpha$)	0.71073	0.71073
2θ range [°]	4.968 to 59.324	6.982 to 154.132
Index ranges	-27 ≤ h ≤ 31, -21 ≤ k ≤ 18, -25 ≤ l ≤ 24	-28 ≤ h ≤ 29, -19 ≤ k ≤ 18, -18 ≤ l ≤ 23
Refl. collected	35911	18489
Independent reflections	7773 [Rint = 0.0635, Rsigma = 0.0598]	6592 [R_{int} = 0.0311, R_{sigma} = 0.0272]
Data/restr./param.	7773/0/370	6592/0/370
Goodness-of-fit on F^2	1.047	1.106
R_1/wR_2[$I > 2\sigma(I)$]	R1 = 0.0387, wR2 = 0.0744	R_1 = 0.0259, wR_2 = 0.0660

Table 3 Selected bond lengths [Å] and bond angles [°] for **1** and **2.**

Bond distances	**1**		**2**
Pd1-Br1	2.4577(4)	Pt1-Br1	2.4625(3)
Pd1-Br2	2.4973(4)	Pt1-Br2	2.4912(3)
Pd1-P2	2.2262(8)	Pt1-P1	2.2055(7)
Pd1-C1	2.105(3)	Pt1-C1	2.086(3)

O1-C2	1.233(4)	O1-C2	1.224(4)
C1-C2	1.490(4)	C1-C2	1.506(4)
P1-C1	1.782(3)	P2-C1	1.792(3)
P1-C10	1.802(3)	P1-C22	1.853(3)
Bond angles			
Br2-Pd1-Br1	92.594(13)	Br2-Pt1-Br1	91.022(12)
C1-Pd1-P2	89.14(9)	C1-Pt1-P1	89.92(8)
C1-Pd1-Br1	172.53(8)	C1-Pt1-Br2	91.47(8)
P2-Pd1-Br1	86.91(2)	P1-Pt1-Br1	88.35(2)
P2-Pd1-Br2	170.29(2)	P1-Pt1-Br2	171.054(19)

Table 4 Selected bond lengths (Å) and bond angles (˚) of [$YMBr_2$](M=Pd, Pt; Y=Y^1, Y^2) complexes at the BP86/def2-SVP level of theory. (The values given in parentheses are the corresponding to the experimental data).

	[Y^1PdBr_2]	**[Y^2PdBr_2]**	**[Y^1PtBr_2]**	**[Y^2PtBr_2]**
	Bond Lengths (Å)	Bond Lengths (Å)	Bond Lengths (Å)	Bond Lengths (Å)

M−C(ylide)	2.14(2.10)	2.15	2.13(2.09)	2.14
M−P	2.27(2.23)	2.29	2.25(2.20)	2.26
M−Br	2.49(2.50)	2.49	2.51(2.49)	2.51
	Bond angle (˚)	Bond angle (˚)	Bond angle (˚)	Bond angle (˚)
P−M−C	90.77(89.2)	96.49	90.75(89.92)	96.81
Br−M−Br	92.78(92.59)	88.92	90.99(91.02)	88.78
P−M−Br	87.71(86.94)	87.05	90.15(88.35)	88.94
C−M−Br	89.47(92.35)	87.65	88.57(91.48)	88.62

Table 5 EDA (BP86/SVP(ZORA)//BP86/def2-SVP) of [$YMBr_2$](M=Pd, Pt Y=Y^1, Y^2) complexes with the C1 symmetry.

Parameter	**[Y^1PdBr_2]**	**[Y^1PtBr_2]**	**[Y^2PdBr_2]**	**[Y^2PtBr_2]**
ΔE int	-116.36	-150.29	-120.03	-151.52
ΔEpauli	267.36	344.69	258.48	332.92
ΔEelast	-222.50(57.9)	-287.57(58.1)	-216.16	-277.51(57.3)
ΔEorb	-141.02(36.7)	-181.98(36.7)	-141.19	-180.39(37.2)
ΔEdis	-20.20(5.4)	-25.44(5.2)	-21.16	-26.54(5.5)
ΔEorb, σd	-72.57(61.3)	-83.72(54.3)	-71.92	-82.18(54.4)
ΔEorb, σd	-18.55(15.7)	-36.50(23.7)	-20.05	-37.99(25.2)
ΔEorb, $\pi^{\perp}$	-11.76(9.9)	-14.52(9.4)	-9.28	-12.12(8.1)
ΔEorb, $\pi^{\parallel}$	-8.51(7.3)	-12.30(8.0)	-9.36	-12.97(8.6)
ΔEorb, $\pi^{\perp}$	-6.91(5.8)	-7.16(4.6)	-5.67	-5.65(3.7)
ΔEorb, rest	-10.89	-12.74	-9.57	-12.63

Table 6 Average inhibition zone of the evaluated bacteria against the newly synthesized complexes.

Sample	**Concentration (mg ml^{-1})**	***S. aureus* (+)**	***B. cereus* (+)**	***E. coli* (-)**	***P. aeruginosa* (-)**
1	**0.5 mg ml^{-1}**	12.33^{a}±0.57	NA	10.67^{b}±0.57	NA
	1 mg ml^{-1}	12.67^{a}±1.15	NA	13.33^{a}±1.52	NA
2	**0.5 mg ml^{-1}**	NA	NA	NA	11.64^{a}±0.57
	1 mg ml^{-1}	NA	11^{b}±1	NA	14.67^{a}±0.57
3	**0.5 mg ml^{-1}**	19.6^{a}±0.35	14.67^{b}±0.5	7.33^{c}±0.57	14.33^{b}±0.5
	1 mg ml^{-1}	19.67^{a}±0.57	17.67^{b}±0.5	7.67^{d}±0.54	14.6^{c}±0.57
4	**0.5 mg ml^{-1}**	NA	9.33^{a}±0.58	8.7^{a}±0.42	NA
	1 mg ml^{-1}	12.61^{a}±0.58	10.67^{b}±0.57	9.1^{b}±0.51	NA

Experiment was performed in triplicate and expressed as mean ± SD. Values in each column with different superscripts are significantly different (P< 0.05).NA: No Active.

Table 7 Antibacterial activity of the antibiotics (positive controls) and DMSO (negative control).

Microorganism	Inhibition zone (mm)				
	Positive control				Negative control
	Gentamicin	**Penicillin**	**Nitrofurantoin**	**Neomycin**	**DMSO**
S.aureus (+)	35 ± 0.24	Na	30 ± 0.34	25 ± 0.45	NA
B. cereus (+)	25 ± 0.18	Na	10 ± 0.12	20 ± 0.36	NA
E. coli (-)	Na	Na	25 ± 0.22	20 ± 0.33	NA
P.aeruginosa (−)	33 ± 0.34	NA	11 ± 0.12	17± 0.12	NA

Experiment was performed in triplicate and expressed as mean ± SD. Values in each column with different superscripts are significantly different ($P< 0.05$).NA: No Active.

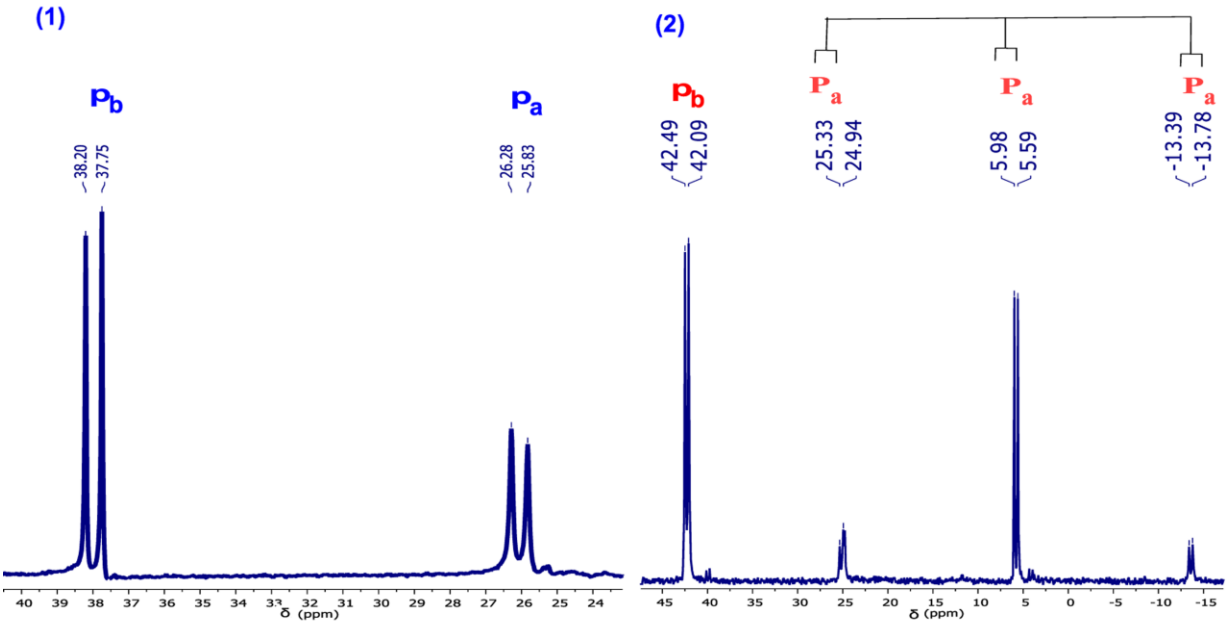

fig 1

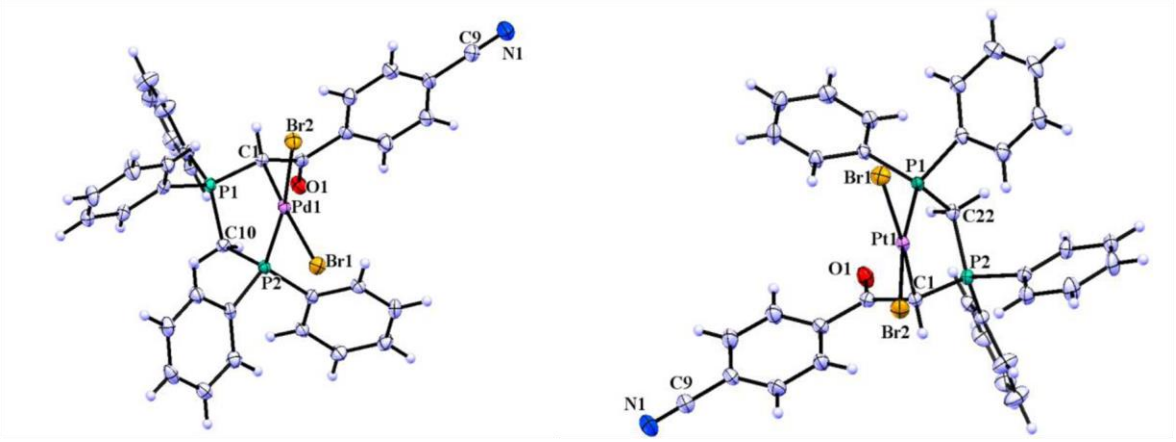

fig 2

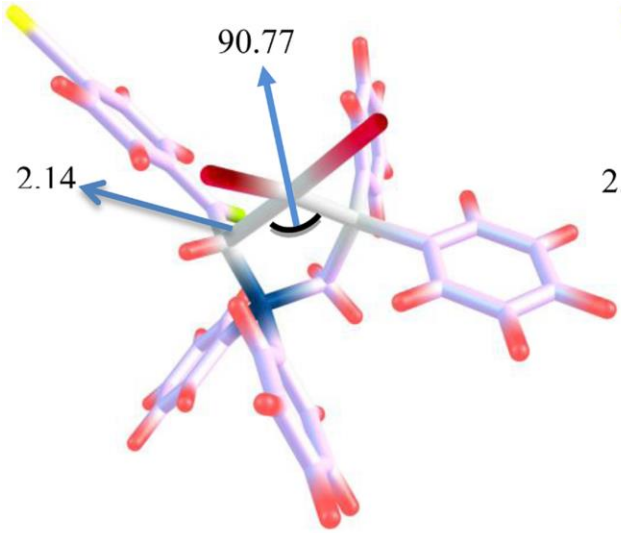

$[PdBr_2Y^1]$

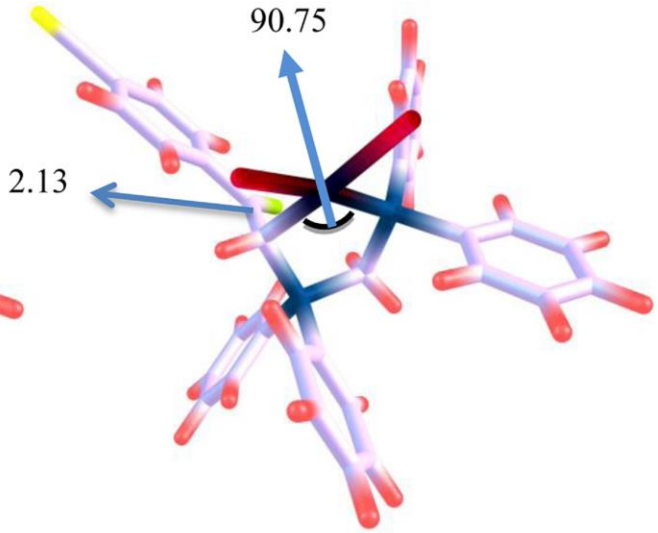

$[PtBr_2Y^1]$

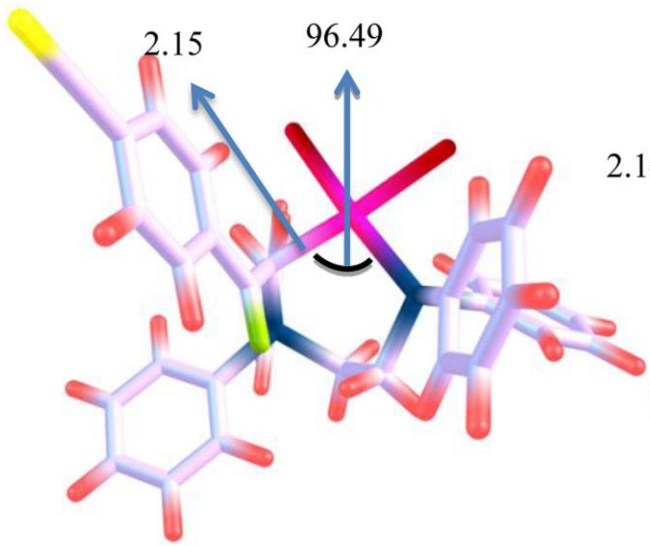

$[PdBr_2Y^2]$

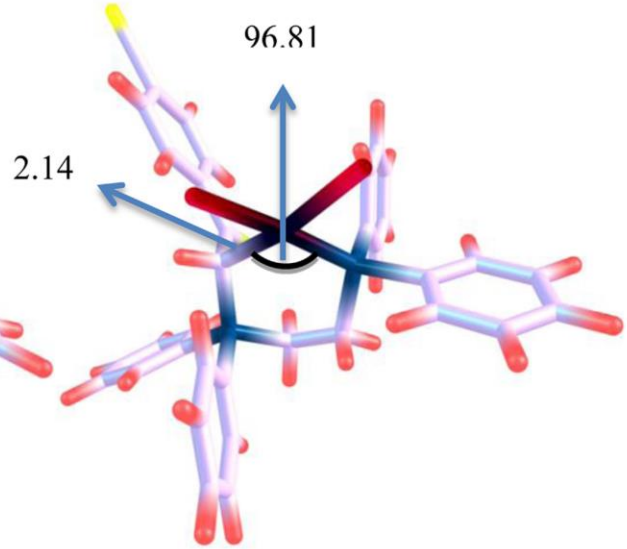

$[PtBr_2Y^2]$

fig 3

[Y^1PdBr_2]		[Y^2PdBr_2]	
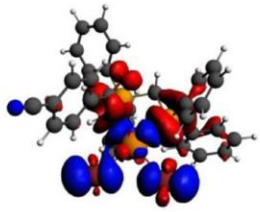	Δρ1: ΔE= -72.57, ν= 1.20 Contour=0.001	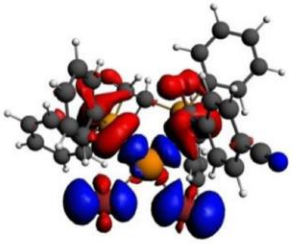	Δρ1: ΔE -71.92, ν= 1.20 Contour=0.001
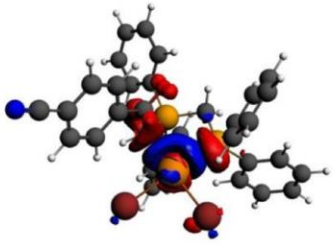	Δρ2: ΔE= -18.52, ν= 0.383 Contour=0.0008	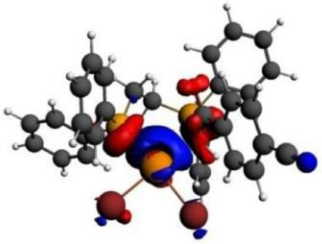	Δρ2: ΔE= -20.05, ν= 0.40 Contour=0.0005
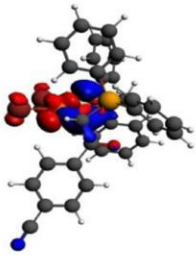	Δρ3: ΔE= -11.76, ν= 0.348 Contour=0.0005	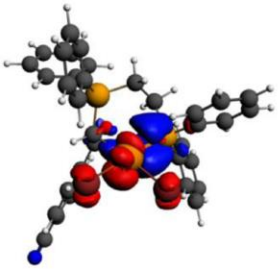	Δρ3: ΔE= -9.28, ν= 0.311 Contour=0.0005
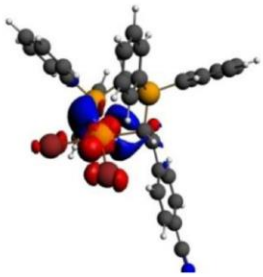	Δρ4: ΔE= -8.51, ν= 0.285 Contour=0.003	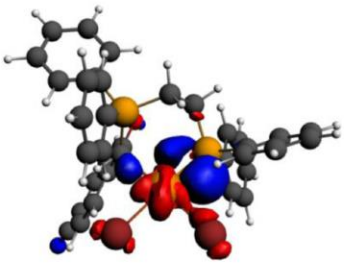	Δρ4: ΔE= -9.36, ν= 0.281 Contour=0.0005
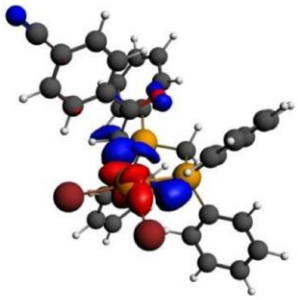	Δρ5: ΔE= -6.91 ν= 0.253 Contour=0.0005	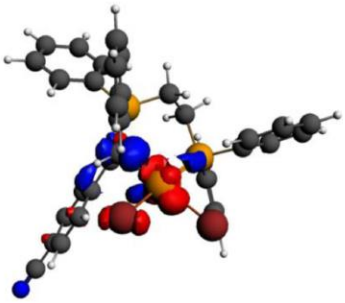	Δρ5: ΔE= -5.67 ν= 0.246 Contour=0.0005
ΔErest= -10.71		ΔErest= -9.57	

fig 4

[Y^1PtBr_2]		[Y^2PtBr_2]	
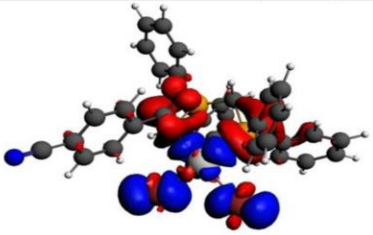	Δρ1: ΔE= -83.72, ν= 1.15 Contour=0.001	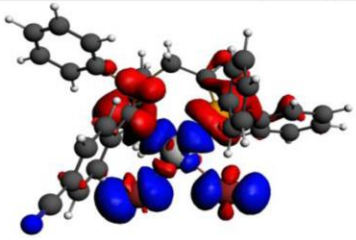	Δρ1: ΔE= -82.18, ν= 1.15 Contour=0.001
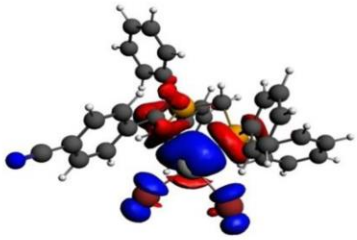	Δρ2: ΔE= -36.50, ν= 0.546 Contour=0.001	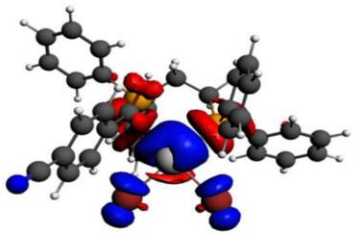	Δρ2: ΔE= -37.99, ν= 0.56 Contour=0.001
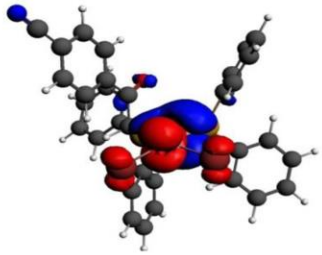	Δρ3: ΔE= -14.52, ν= 0.40 Contour=0.0003	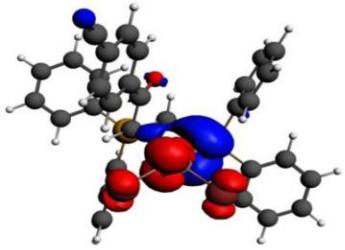	Δρ3: ΔE= -12.12, ν= 0.36 Contour=0.0005
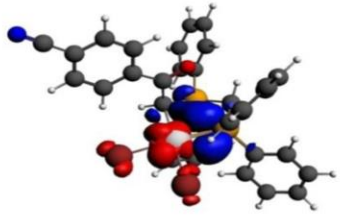	Δρ4: ΔE= -12.30, ν= 0.33 Contour=0.0005	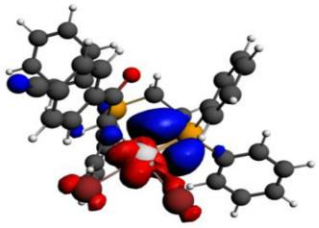	Δρ4: ΔE= -12.97, ν= 0.33 Contour=0.0005
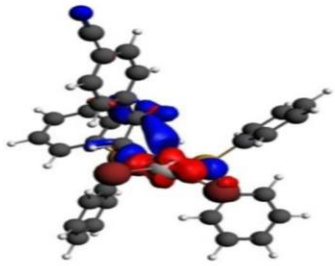	Δρ5: ΔE= -7.16, ν= 0.28 Contour=0.0001	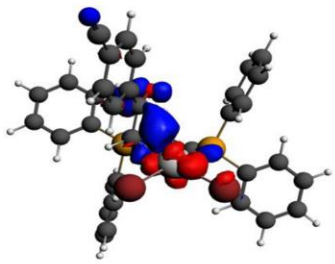	Δρ5: ΔE= -5.65, ν= 0.27 Contour=0.0008
ΔErest= -12.74		ΔErest= -12.63	

fig 5

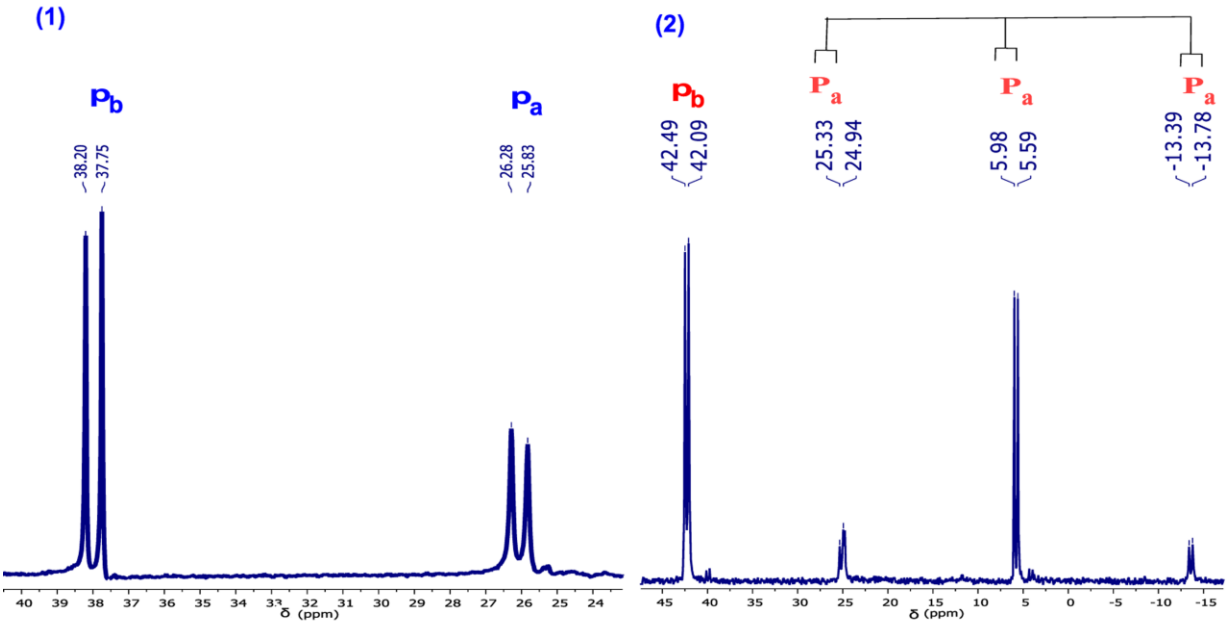

fig 1

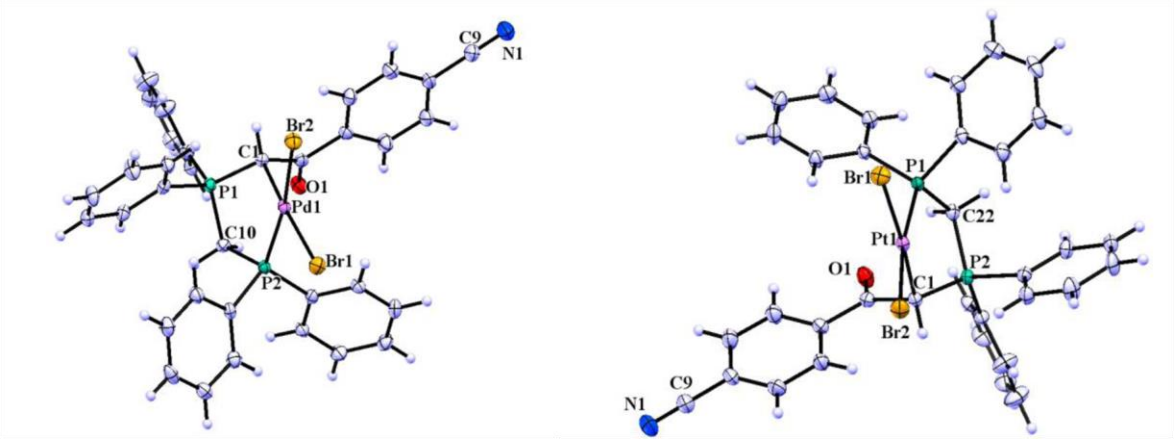

fig 2

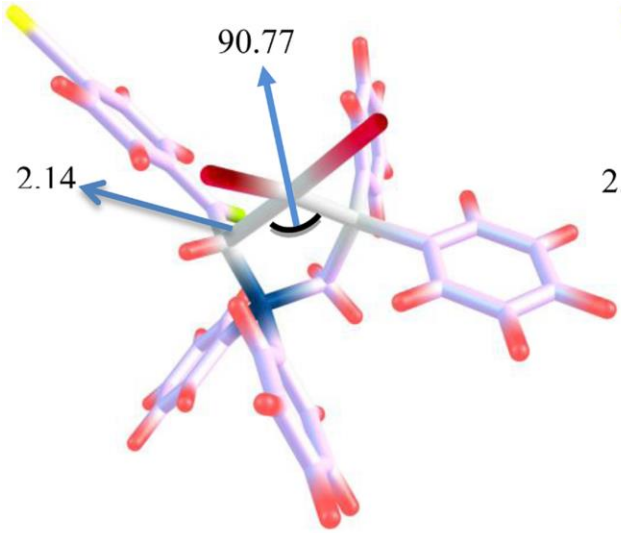

$[PdBr_2Y^1]$

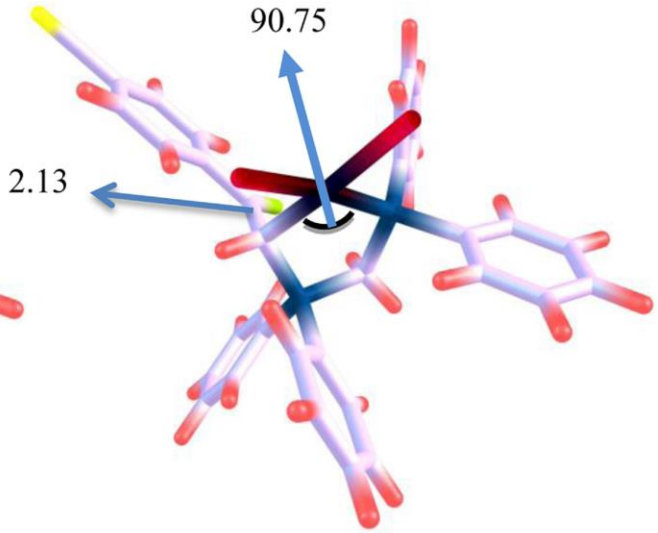

$[PtBr_2Y^1]$

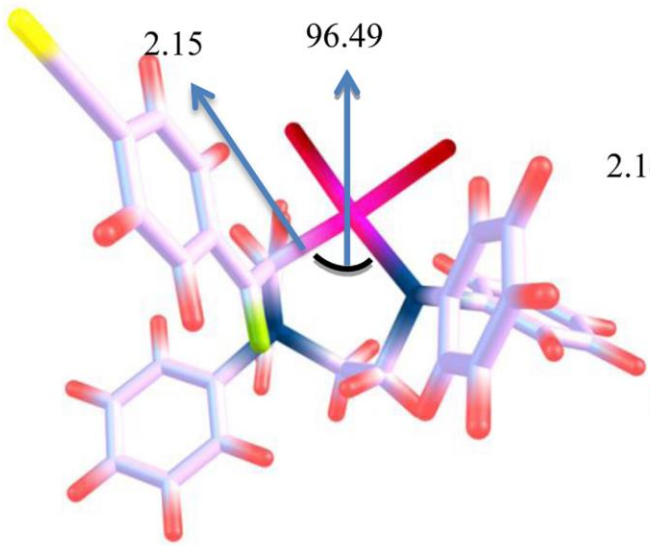

$[PdBr_2Y^2]$

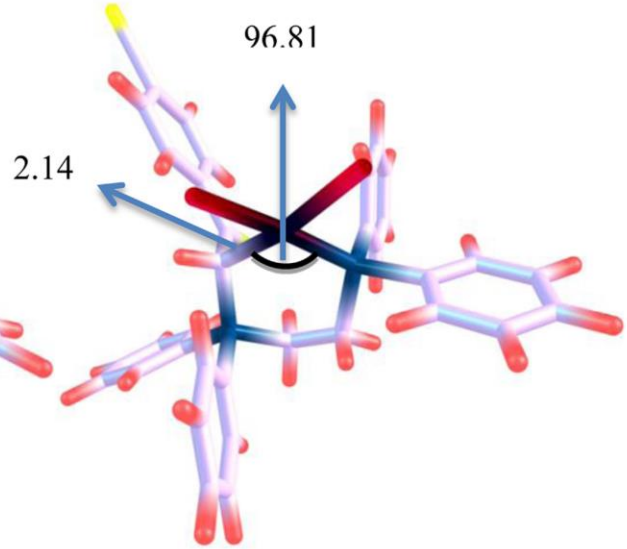

$[PtBr_2Y^2]$

fig 3

[Y^1PdBr_2]		[Y^2PdBr_2]	
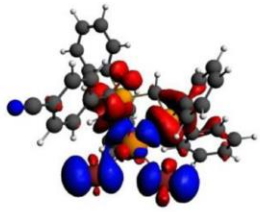	Δρ1: ΔE= -72.57, ν= 1.20 Contour=0.001	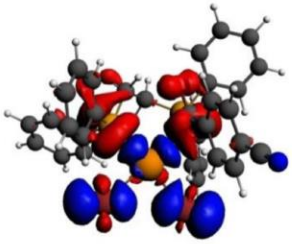	Δρ1: ΔE -71.92, ν= 1.20 Contour=0.001
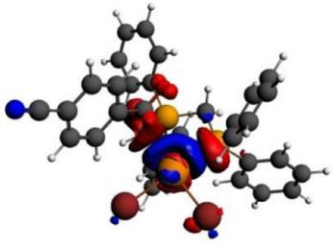	Δρ2: ΔE= -18.52, ν= 0.383 Contour=0.0008	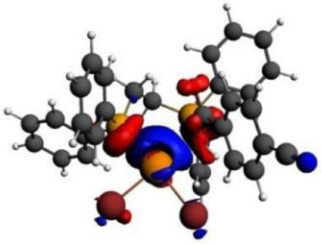	Δρ2: ΔE= -20.05, ν= 0.40 Contour=0.0005
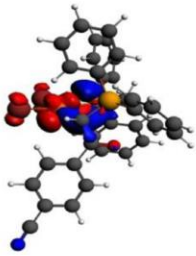	Δρ3: ΔE= -11.76, ν= 0.348 Contour=0.0005	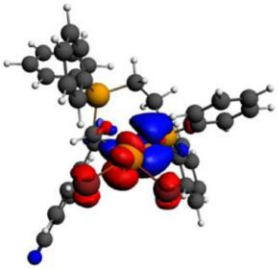	Δρ3: ΔE= -9.28, ν= 0.311 Contour=0.0005
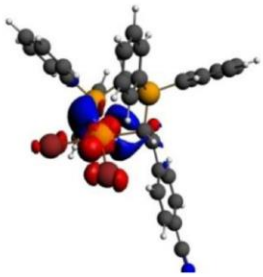	Δρ4: ΔE= -8.51, ν= 0.285 Contour=0.003	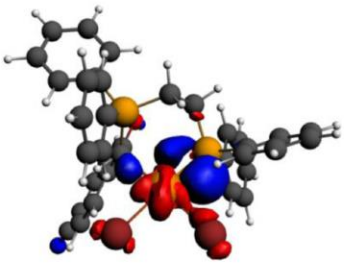	Δρ4: ΔE= -9.36, ν= 0.281 Contour=0.0005
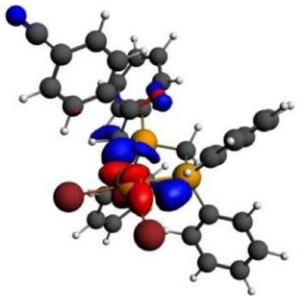	Δρ5: ΔE= -6.91 ν= 0.253 Contour=0.0005	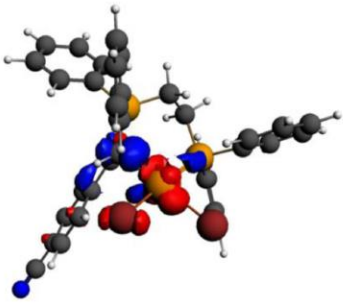	Δρ5: ΔE= -5.67 ν= 0.246 Contour=0.0005
ΔErest= -10.71		ΔErest= -9.57	

fig 4

[Y^1PtBr_2]		[Y^2PtBr_2]	
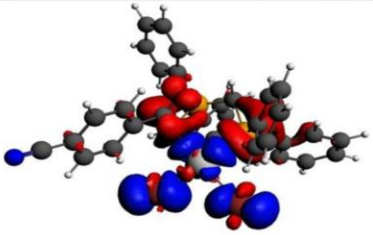	Δρ1: ΔE= -83.72, ν= 1.15 Contour=0.001	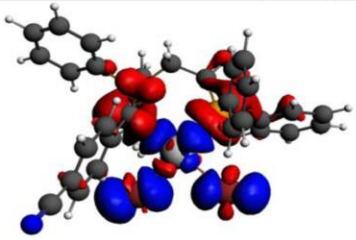	Δρ1: ΔE= -82.18, ν= 1.15 Contour=0.001
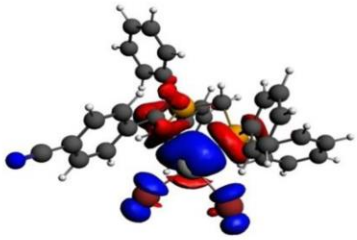	Δρ2: ΔE= -36.50, ν= 0.546 Contour=0.001	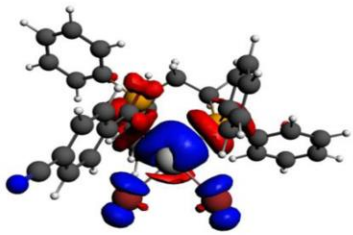	Δρ2: ΔE= -37.99, ν= 0.56 Contour=0.001
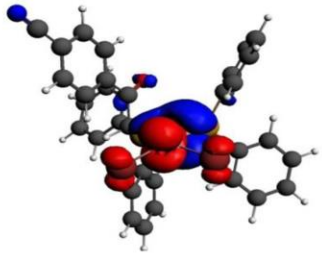	Δρ3: ΔE= -14.52, ν= 0.40 Contour=0.0003	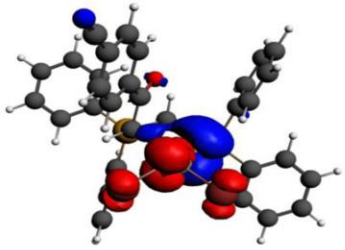	Δρ3: ΔE= -12.12, ν= 0.36 Contour=0.0005
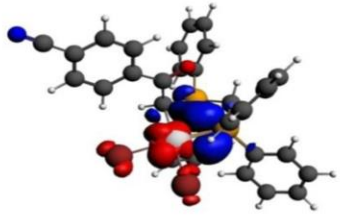	Δρ4: ΔE= -12.30, ν= 0.33 Contour=0.0005	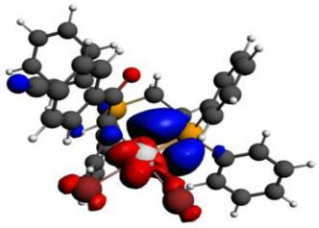	Δρ4: ΔE= -12.97, ν= 0.33 Contour=0.0005
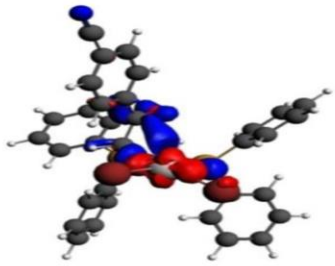	Δρ5: ΔE= -7.16, ν= 0.28 Contour=0.0001	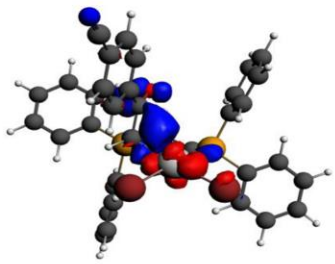	Δρ5: ΔE= -5.65, ν= 0.27 Contour=0.0008
ΔErest= -12.74		ΔErest= -12.63	

fig 5

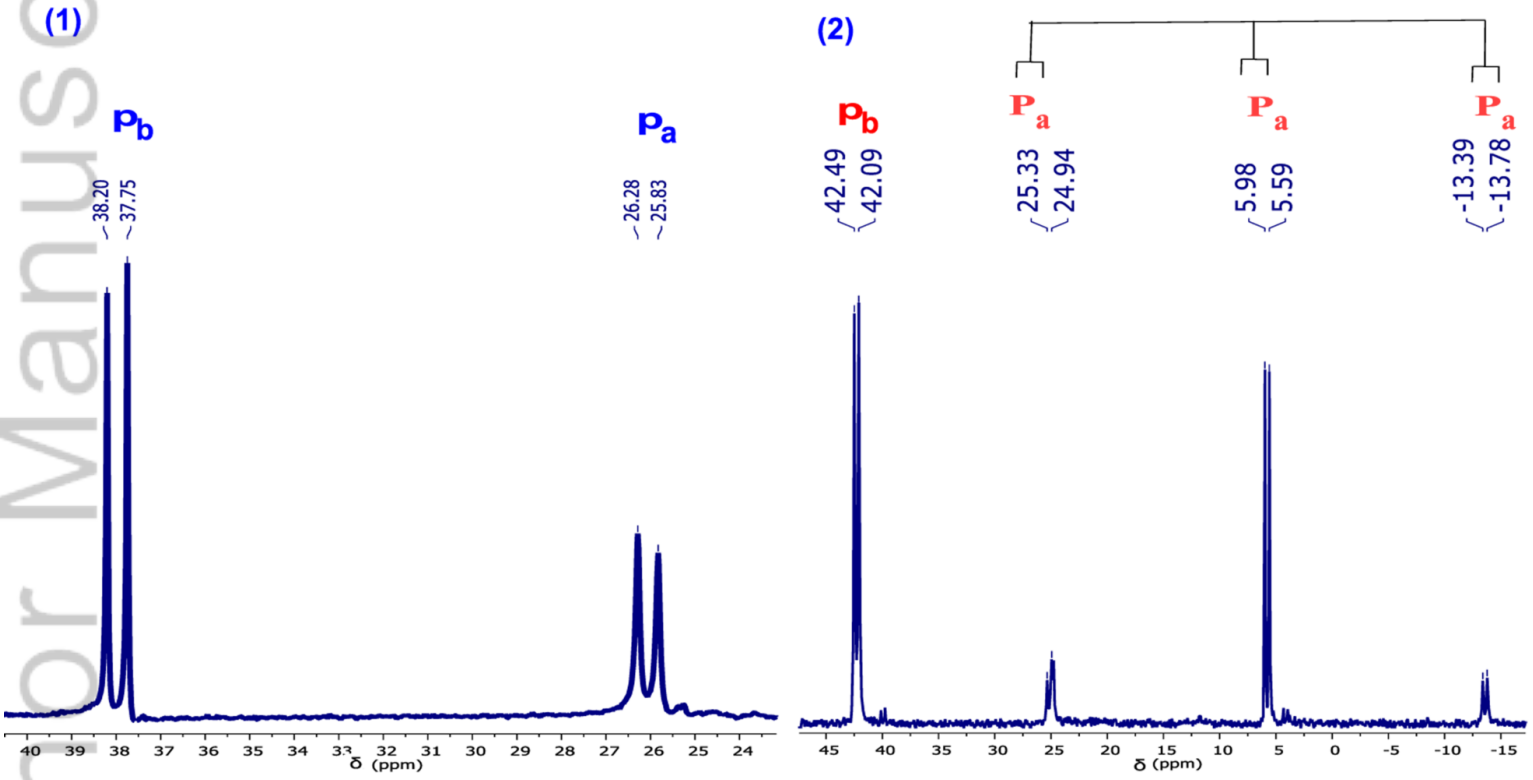

AOC_4658_F1.tif

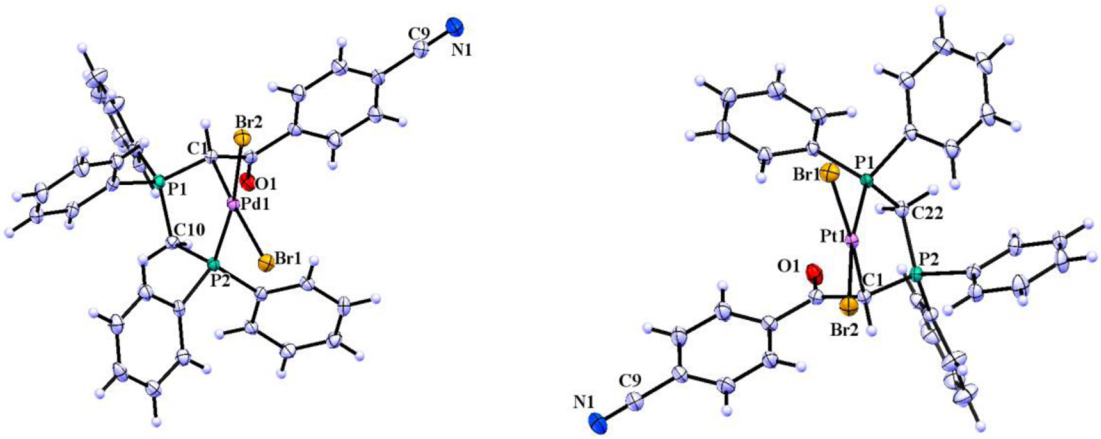

AOC_4658_F2.tif

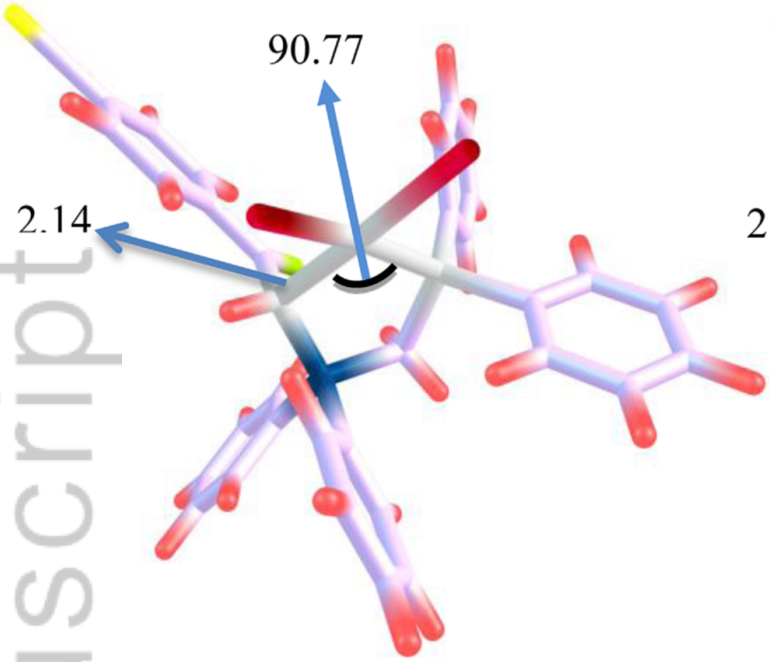

$[PdBr_2Y^1]$

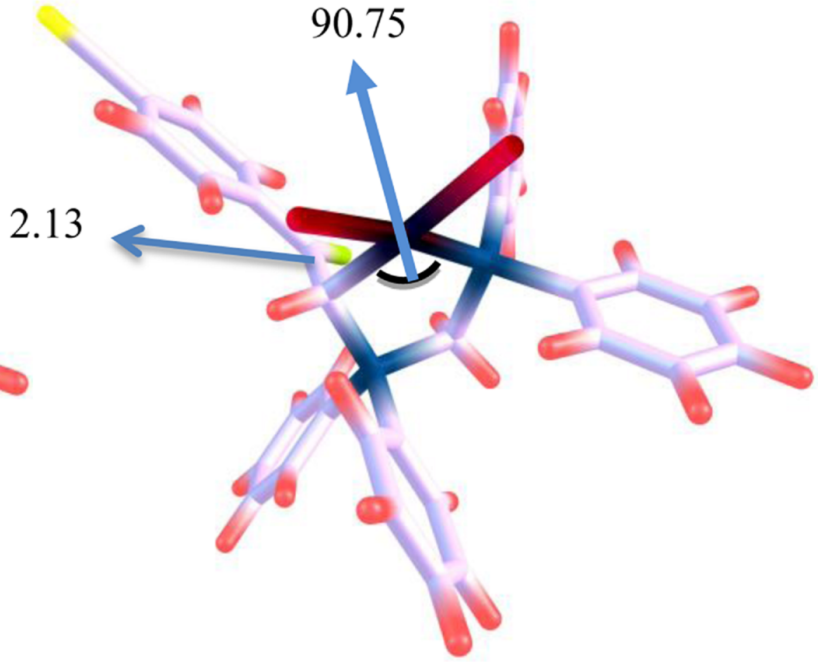

$[PtBr_2Y^1]$

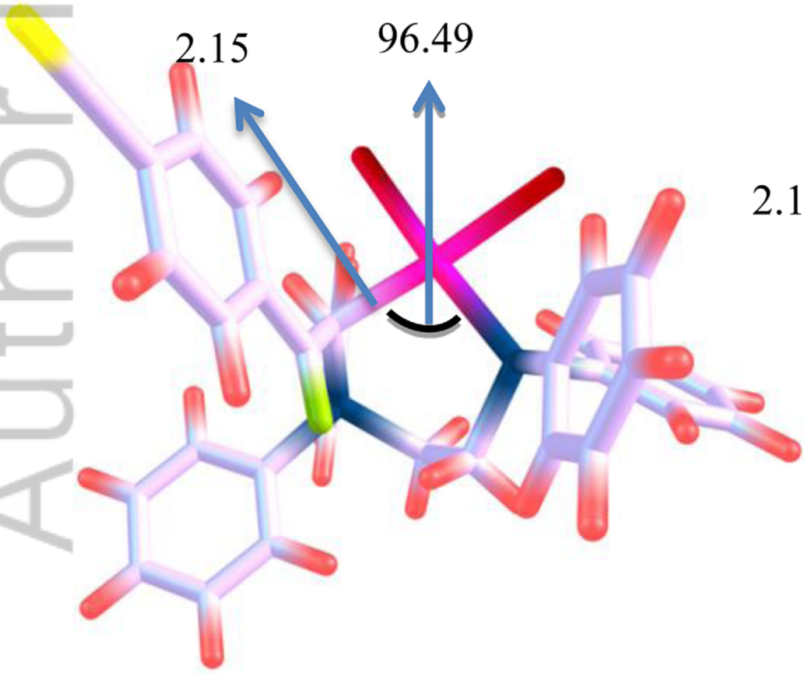

$[PdBr_2Y^2]$

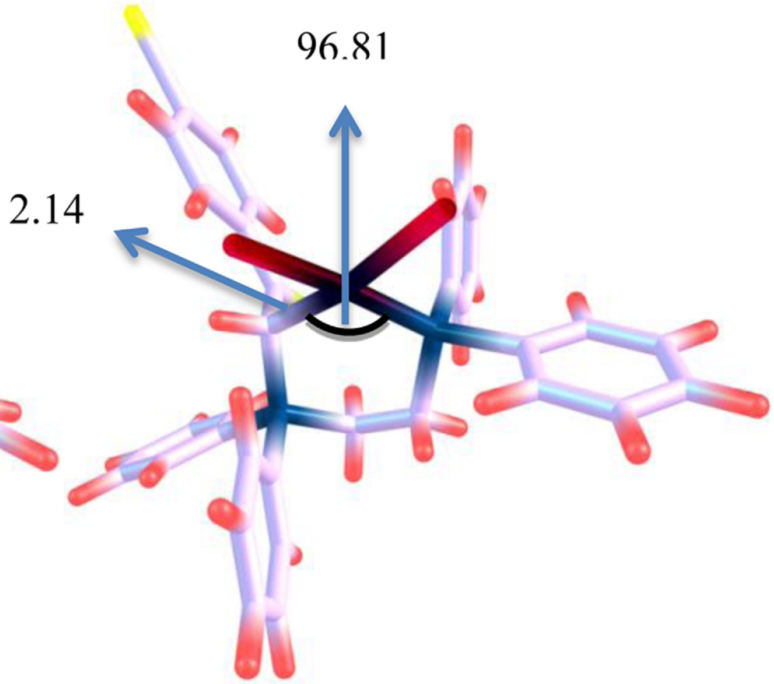

$[PtBr_2Y^2]$

AOC_4658_F3.tif

[Y^1PdBr_2]		[Y^2PdBr_2]	
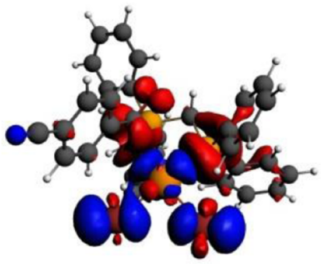	Δρ1: ΔE= -72.57, ν= 1.20 Contour=0.001	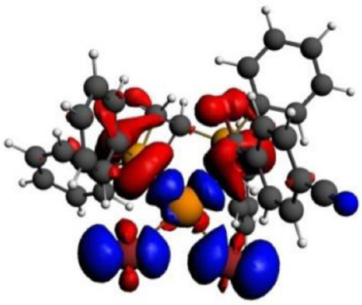	Δρ1: ΔE -71.92, ν= 1.20 Contour=0.001
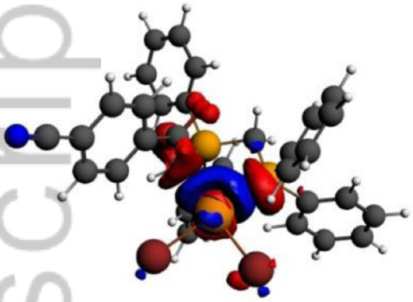	Δρ2: ΔE= -18.52, ν= 0.383 Contour=0.0008	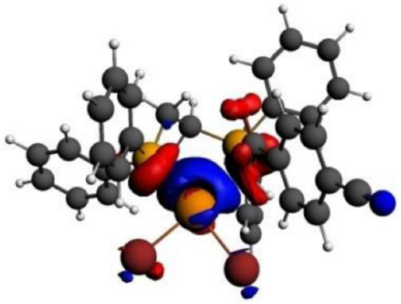	Δρ2: ΔE= -20.05, ν= 0.40 Contour=0.0005
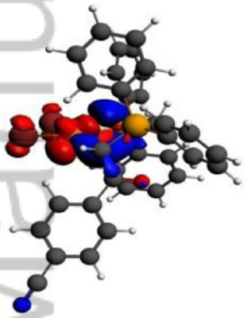	Δρ3: ΔE= -11.76, ν= 0.348 Contour=0.0005	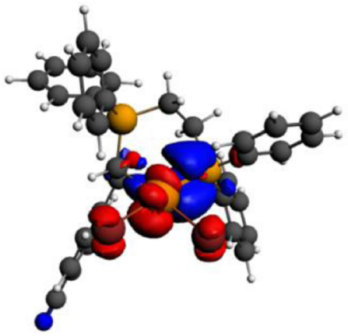	Δρ3: ΔE= -9.28, ν= 0.311 Contour=0.0005
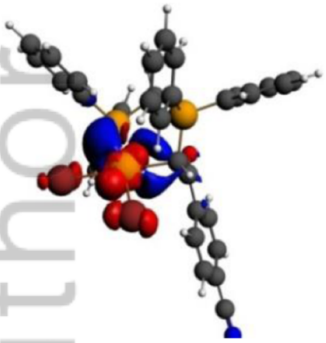	Δρ4: ΔE= -8.51, ν= 0.285 Contour=0.003	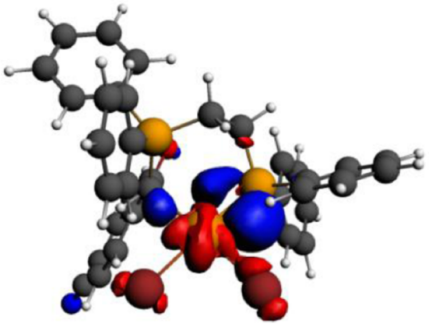	Δρ4: ΔE= -9.36, ν= 0.281 Contour=0.0005
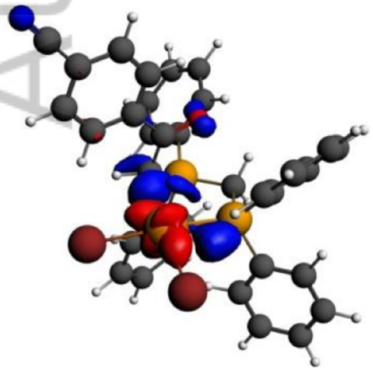	Δρ5: ΔE= -6.91 ν= 0.253 Contour=0.0005	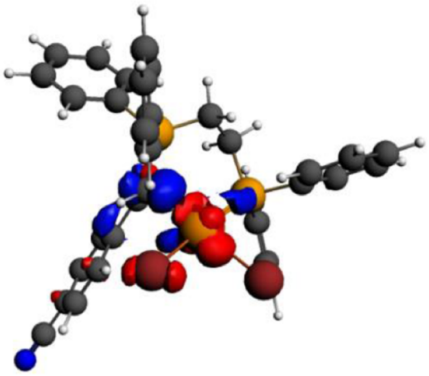	Δρ5: ΔE= -5.67 ν= 0.246 Contour=0.0005
ΔErest= -10.71		ΔErest= -9.57	

[Y^1PtBr_2]		[Y^2PtBr_2]	
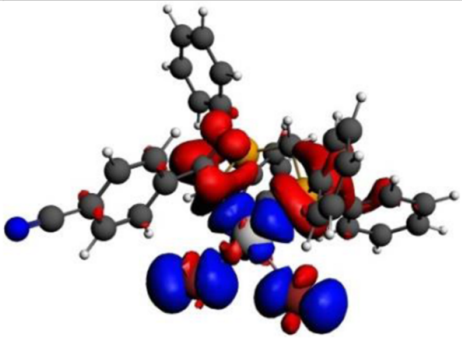	Δρ1: ΔE= -83.72, ν= 1.15 Contour=0.001	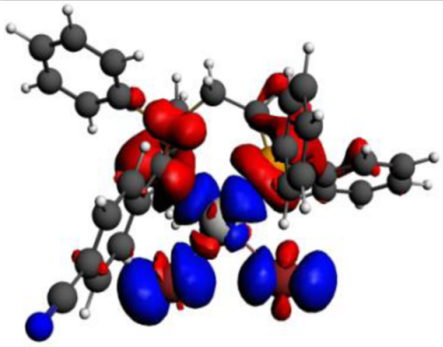	Δρ1: ΔE= -82.18, ν= 1.15 Contour=0.001
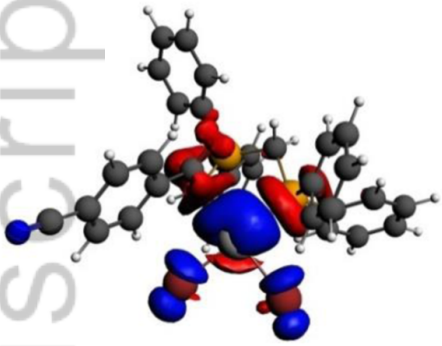	Δρ2: ΔE= -36.50, ν= 0.546 Contour=0.001	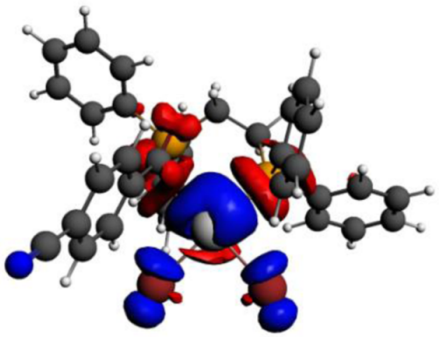	Δρ2: ΔE= -37.99, ν= 0.56 Contour=0.001
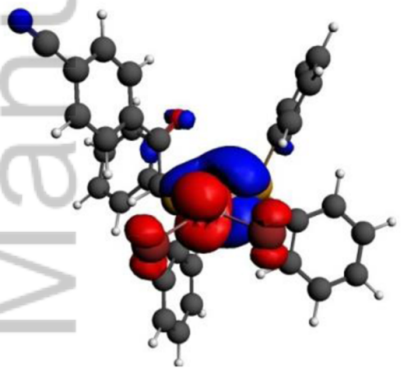	Δρ3: ΔE= -14.52, ν= 0.40 Contour=0.0003	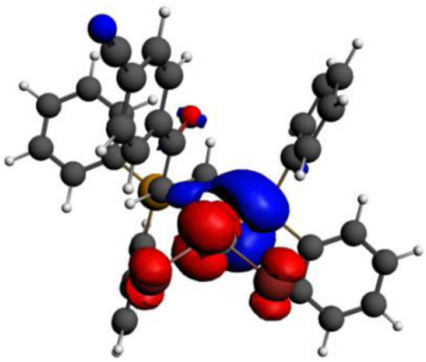	Δρ3: ΔE= -12.12, ν= 0.36 Contour=0.0005
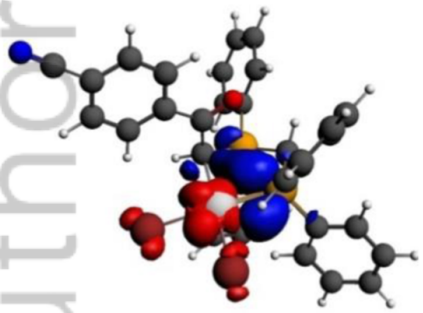	Δρ4: ΔE= -12.30, ν= 0.33 Contour=0.0005	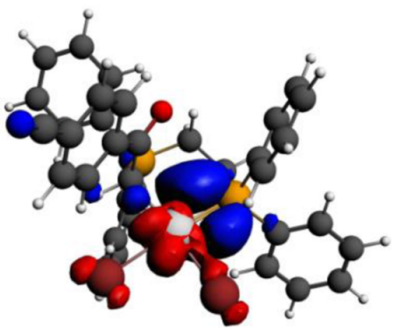	Δρ4: ΔE= -12.97, ν= 0.33 Contour=0.0005
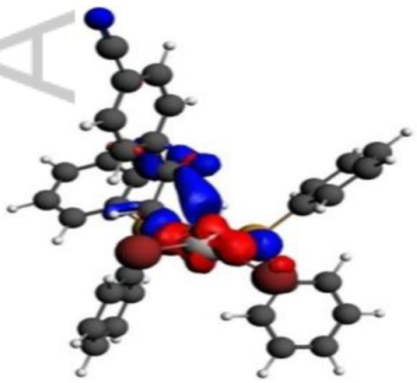	Δρ5: ΔE= -7.16, ν= 0.28 Contour=0.0001	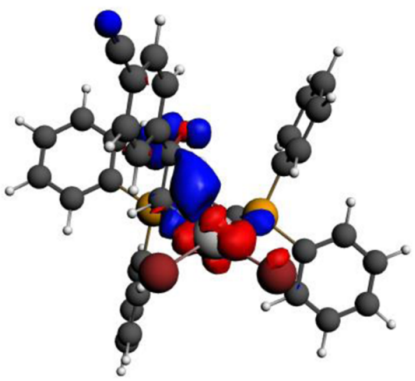	Δρ5: ΔE= -5.65, ν= 0.27 Contour=0.0008
ΔErest= -12.74		ΔErest= -12.63	

AOC_4658_F5.tif

FIGURE 1: The 31P NMR spectra of complexes 1 and 2.

FIGURE 2: ORTEP view of X-ray crystal structure 1 and 2.

FIGURE 3: Optimized structures of [YMBr2](M=Pd, Pt Y=Y1, Y2) complexes at the BP86/SVP level of theory. Bond lengths are given in Å, bond angles in degrees.

FIGURE 4: Deformation densities associated with the most important orbital interactions for [YPdBr2](Y=Y1, Y2) complexes.

FIGURE 5: Deformation densities associated with the most important orbital interactions for [YPtBr2](Y=Y1, Y2) complexes.

SCHEME 1 Synthesis of Y1, Y2and Pt/Pd complexes 1-4.

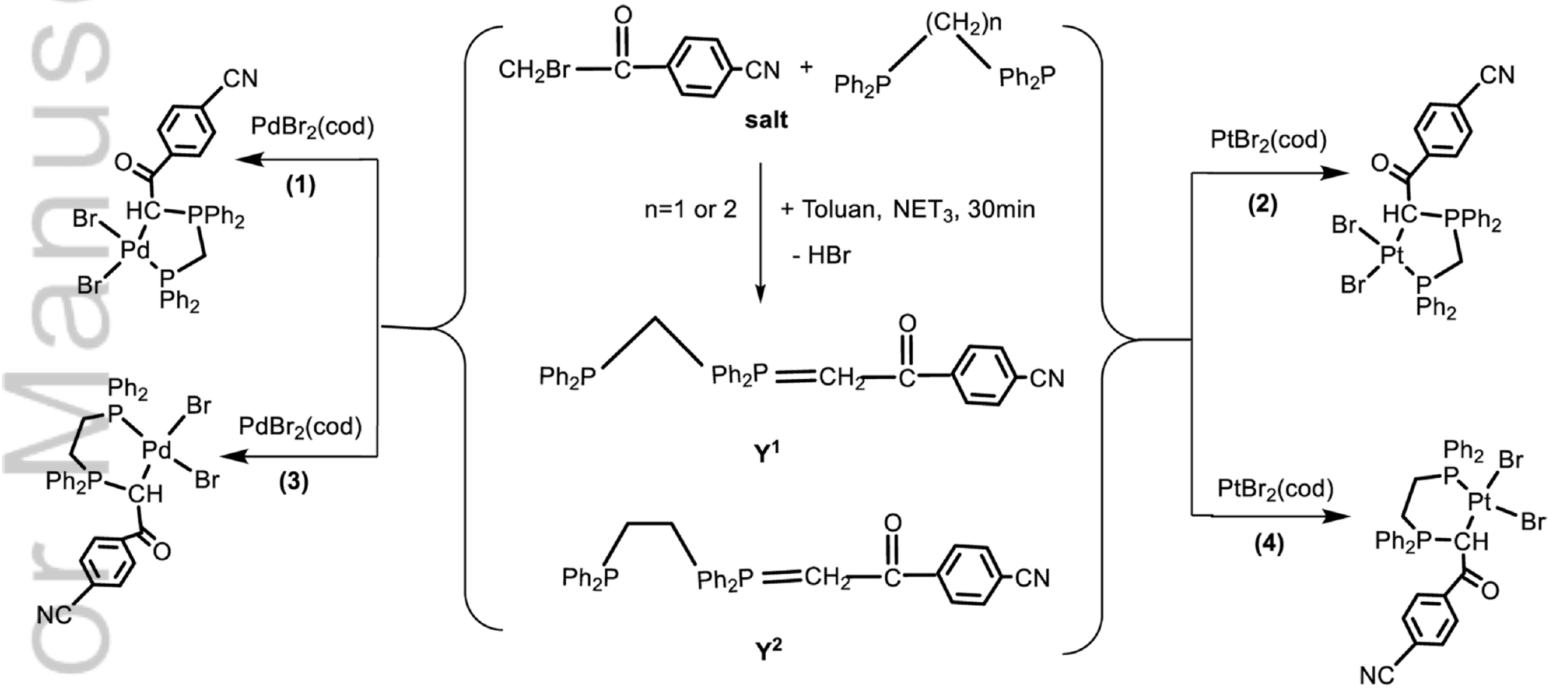

AOC_4658_Schem1 (1).tif

Author/s:
Sabounchei, SJ; Badpa, K; Bayat, M; Karamian, R; Ghasemlou, F; Gable, RW; Derakhshandeh, PG; Van Hecke, K

Title:
Spectral, crystallographic, theoretical and antibacterial studies of palladium(II)/platinum(II) complexes with unsymmetric diphosphine ylides

Date:
2019-03-01

Citation:
Sabounchei, S. J., Badpa, K., Bayat, M., Karamian, R., Ghasemlou, F., Gable, R. W., Derakhshandeh, P. G. & Van Hecke, K. (2019). Spectral, crystallographic, theoretical and antibacterial studies of palladium(II)/platinum(II) complexes with unsymmetric diphosphine ylides. APPLIED ORGANOMETALLIC CHEMISTRY, 33 (3), https://doi.org/10.1002/aoc.4658.

Persistent Link:
http://hdl.handle.net/11343/284903

File Description:
Accepted version